International Union of
Pure and Applied Chemistry

ICPOC 24: Fornarini S: Binding motifs of cisplatin interaction with simple biomolecules and aminoacid targets probed by IR ion spectroscopy

Journal:	*Pure and Applied Chemistry*
Manuscript ID	PAC-CON-19-01-10.R1
Manuscript Type:	Conference
Date Submitted by the Author:	n/a
Complete List of Authors:	Corinti, Davide; Università degli Studi di Roma La Sapienza, Dipartimento di Chimica e Tecnologie del Farmaco Paciotti, Roberto; Università G. D'Annunzio Chieti-Pescara, Dipartimento di Farmacia Re, Nazzareno; Università G. D'Annunzio Chieti-Pescara, Dipartimento di farmacia Coletti, Cecilia; Università G. D'Annunzio Chieti-Pescara, Dipartimento di farmacia Chiavarino, Barbara; Università degli Studi di Roma La Sapienza, Dipartimento di Chimica e Tecnologie del Farmaco Crestoni, Maria Elisa; Università degli Studi di Roma La Sapienza, Dipartimento di Chimica e Tecnologie del Farmaco Fornarini, Simonetta; Università degli Studi di Roma La Sapienza, Dipartimento di Chimica e Tecnologie del Farmaco
Keywords:	cisplatin, transplatin, IRMPD spectroscopy, photofragmentation kinetics, ligand substitution
Author-Supplied Keywords:	

Davide Corinti, Roberto Paciotti, Nazzareno Re, Cecilia Coletti, Barbara Chiavarino, Maria Elisa Crestoni and Simonetta Fornarini*

Binding motifs of cisplatin interaction with simple biomolecules and aminoacid targets probed by IR ion spectroscopy

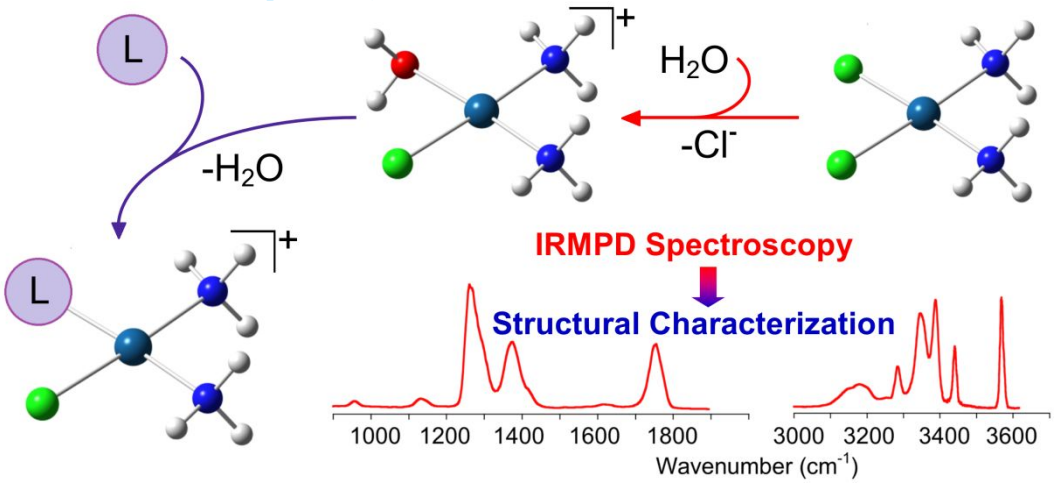

The active aqua derivatives of cisplatin (and transplatin) have been structurally characterized as isolated species, as well as the early substitution complexes with the biological targets.

Davide Corinti, Roberto Paciotti, Nazzareno Re, Cecilia Coletti, Barbara Chiavarino, Maria Elisa Crestoni and Simonetta Fornarini*

Binding motifs of cisplatin interaction with simple biomolecules and aminoacid targets probed by IR ion spectroscopy

Davide Corinti, Barbara Chiavarino, Maria Elisa Crestoni and Simonetta Fornarini: Dipartimento di Chimica e Tecnologie del Farmaco, Università degli Studi di Roma La Sapienza, P.le A. Moro 5, I-00185 Roma, Italy
E-mail: simonetta.fornarini@uniroma1.it

Roberto Paciotti, Nazzareno Re, Cecilia Coletti: Dipartimento di Farmacia
Università G. D'Annunzio Chieti-Pescara, Via dei Vestini 31, I-66100 Chieti, Italy

Abstract: The primary intermediates resulting from the interaction of cisplatin, *cis*-($PtCl_2(NH_3)_2$], most widespread antitumor drug, with biomolecular targets are characterized. Electrospray ionization is used to deliver ions formed in solution into the gas phase where they are structurally interrogated by vibrational "action" spectroscopy in conjunction with quantum chemical calculations. The aquation products, *cis*-$[PtX(NH_3)_2(H_2O)]^+$ (X = Cl, OH), lying along the path responsible for biological activity, are shown to display distinctive features responding to ligation pattern and optimized geometry. The IR spectra of *trans*-$[PtX(NH_3)_2(H_2O)]^+$ are different, testifying that *cis* and *trans* complexes are stable, non interconverting species both in solution and in the gas phase. Ligand substitution by simple nucleophiles (L = pyridine, 4(5)-methylimidazole, thioanisole, trimethylphosphate, acetamide, dimethylacetamide, urea and thiourea) yields *cis*-$[PtCl(NH_3)_2(L)]^+$ complexes displaying remarkable regioselectivity whenever L presents multiple candidate platination sites. The incipient formation of cisplatin-derived complexes with the recognized biological amino acid targets L-histidine (His) and L-methionine (Met) has been investigated revealing the primary platination event to be mainly directed at the N_π atom of the imidazole side chain of His and to the thiomethyl sulfur of Met. The isomer and conformer population of the ensuing *cis*-$[PtCl(NH_3)_2(Met/His)]^+$ complexes, sampled in the gas phase, can be ascertained by photofragmentation kinetics on isomer/conformer specific resonances.

Keywords: cisplatin, transplatin, IRMPD spectroscopy, photofragmentation kinetics, ligand substitution

Introduction

Cisplatin [*cis*-diamminedichloroplatinum(II), A in Scheme 1] is one of the most widely used chemotherapeutic agents for the treatment of various tumors, a position held since several decades (FDA approval dates back to 1978), following the serendipitous discovery of its anticancer activity by Rosenberg in the 1960s [1-2]. Nowadays cisplatin still represents the reference molecule for a large number of platinum(II) and platinum(IV) compounds, being designed and tested for tumor growth inhibition. Binding

of cisplatin to DNA is ultimately responsible for cell death and occurs via stepwise replacement of chlorido ligands by a solvent assisted mechanism [3-6]. Hydrolysis leads to charged complexes such as *cis*-$[PtCl(NH_3)_2(H_2O)]^+$ and *cis*-$[Pt(OH)(NH_3)_2(H_2O)]^+$, prone to react by electrostatic preassociation and nucleophilic substitution of aqua ligand(s) by nucleobases and final crosslink formation. Besides DNA, cisplatin is known to bind proteins and small molecules such as glutathione through sulfur or nitrogen donor moieties [7-9]. Given the high interest attached to cisplatin reactions with biomolecules, a considerable number of mechanistic studies have been devoted to clarify ligand substitution processes of platinum(II) complexes in protic media. However, the ligand substitution reactivity of platinum(II) complexes in protic solvents is rather driven towards the formation of complex mixtures of various species [10-14]. Polynuclear and chelated complexes are formed, depending on pH, which governs prototropic equilibria [15-16]. Thus, picking a single specific species to be assayed for structure and reactivity behavior is typically not an easy task. This goal has attracted our interest, aiming to gain a comprehensive molecular level description of the interactions of cisplatin with biomolecular targets such natural amino acids or simple models thereof, the focus being on the early event of metal ligand bonding. The use of mass spectrometry (MS) together with electrospray ionization (ESI) presents considerable advantages because it allows to extract charged species, which may otherwise be fleeting intermediates in solution, and isolate them in a highly dilute environment. The present study is based mainly on Fourier transform ion cyclotron resonance (FT-ICR) MS coupled with ESI. ESI is well suited to extract and analyze cisplatin-related complexes formed in aqueous solution [17-20], which are then accumulated and driven to the FT-ICR cell. In this environment, minimizing any perturbing influence, cisplatin complexes may be characterized for their bimolecular reactivity by ion-molecule reactions, for their fragmentation behavior by collision induced dissociation MS, and for their structural features by Infra Red Multiple Photon Dissociation (IRMPD) spectroscopy combined with quantum chemical calculations. Indeed, detailed structural information about gaseous charged species is currently available using this "action" IR spectroscopy, based on the photofragmentation process induced by the non-coherent absorption of IR photons in resonance with active vibrational modes [21-27]. A wide variety of transition metal complexes have already been characterized by IRMPD spectroscopy, such as, for example, metastable reduced zinc complexes [28], copper resveratrol complexes [29], Zn-salophen complexes with chemosensing properties [30], besides various complexes presenting amino acids and peptides bound to transition metals [31-35].

In this report three main issues will be covered: (i) an outline of the developing information about structural and reactivity features of simple cisplatin derived complexes through IRMPD spectroscopy; (ii) bonding motifs from cisplatin interaction with histidine; (iii) bonding motifs from cis- and transplatin interaction with methionine. Transplatin [*trans*-diamminedichloroplatinum(II), B in Scheme 1] is not endowed with anticancer activity, due to its higher reactivity, responsible for side reactions, and to its inability to form 1,2-adducts [2]. It provides a useful reference as alternative isomer, though.

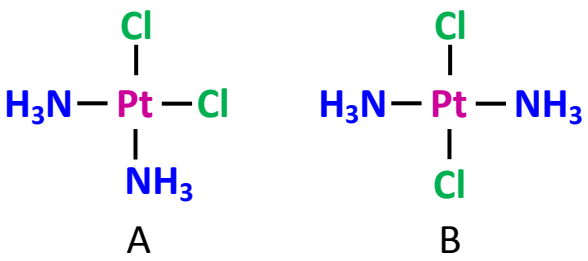

Scheme1: Cisplatin (A) and transplatin (B).

Results and discussion

Cisplatin (and transplatin) aquation and ligand exchange with simple biomolecules

Cisplatin undergoes aquation (replacement of one chlorido ligand with water) in aqueous solution. The controlled hydrolysis, occurring in a suitable time scale preliminarily to DNA binding, is a key step in the antitumor activity. Both singly and diaquated complexes are formed, also the latter believed to contribute to DNA platination which is favored in both cases by the Coulombic interaction of the DNA polyanion with the positively charged complexes. At the same time the charged *cis*-$[PtCl(NH_3)_2(H_2O)]^+$ and *cis*-$[Pt(OH)(NH_3)_2(H_2O)]^+$ complexes are well amenable to ESI-MS analysis allowing them to be characterized by vibrational spectroscopy [36,37]. In their most stable geometry the sampled *cis*-$[PtX(NH_3)_2(H_2O)]^+$ (X = Cl, OH) ions (Fig. 1-2) present the aqua ligand oriented towards X, according to MP2 and DFT calculations. The ensuing hydrogen bonding interaction is responsible for the relatively low frequency of the asymmetric/symmetric OH_2 stretching modes measured experimentally at 3624/3531 and 3600/~~3492~~ 3442 cm^{-1}, for X = Cl and OH, respectively (Fig. 1-2). Incidentally, the evidence obtained by IRMPD experiments needs to be thoroughly examined in parallel with ab initio computations on the candidate species. The selection of the most effective theoretical approach is thus an essential point, as well underlined in the structural determination of a glicine linked cisplatin derivative [38].

Square planar platinum(II) complexes are known to undergo ligand substitution with stereoretention [12]. This notion is confirmed by IRMPD spectroscopy of the aqua complexes formed by hydrolysis of transplatin (Fig. 1-2). In fact, the so-obtained *trans*-$[PtX(NH_3)_2(H_2O)]^+$ (X = Cl, OH) complexes present quite distinct spectra. In particular, the H atoms of the aqua ligand are not engaged in hydrogen bonding which places the asymmetric/symmetric OH_2 stretching modes at 3683/3596 and 3683/3600 cm^{-1}, for X = Cl and OH, respectively. This finding also demonstrates that *cis*-/*trans*-$[PtX(NH_3)_2(H_2O)]^+$ complexes are stable, non interconverting species in the gas phase. Interestingly, the photofragmentation process releases water and the rate of *trans*-$[PtX(NH_3)_2(H_2O)]^+$ isomers is an order of magnitude higher than for the cis counterparts. This result may be viewed as illustration of the trans effect exerted by a trans ligand in labilizing a leaving group departure, which agrees with the order $Cl^- > NH_3$ [2,12,39].

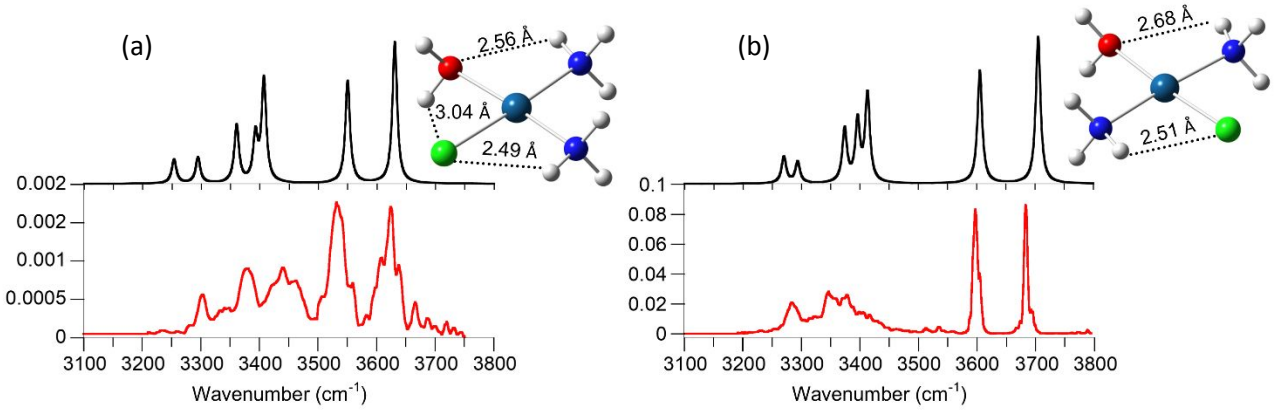

Fig. 1: Experimental IRMPD spectra of *cis*-$[PtCl(NH_3)_2(H_2O)]^+$ (a) and *trans*-$[PtCl(NH_3)_2(H_2O)]^+$ (b) (red profiles) compared with calculated harmonic IR spectra (black profiles) of optimized structures (top right) at MP2/cc-pVTZ (Pt = LANL2TZ) level of theory. Theoretical spectra are scaled by a 0.957 factor.

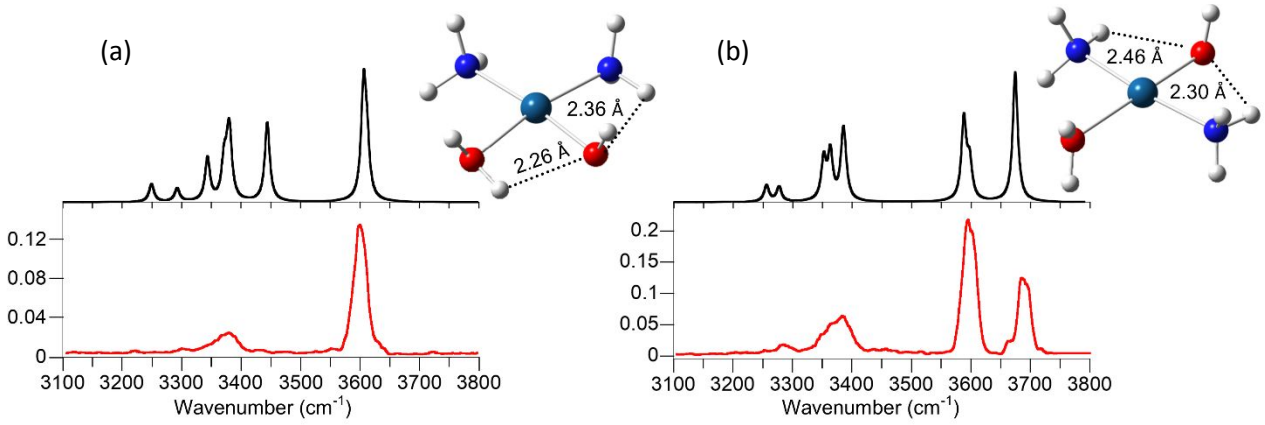

Fig. 2: Experimental IRMPD spectra of *cis*-$[Pt(OH)(NH_3)_2(H_2O)]^+$ (a) and *trans*-$[Pt(OH)(NH_3)_2(H_2O)]^+$ (b) (red profiles) compared with calculated harmonic IR spectra (black profiles) of optimized structures (top right) at B3LYP/cc-pVTZ (Pt = aug-cc-pVTZ-PP) level of theory. Theoretical spectra are scaled by a 0.957 factor.

In the biological environment and along the path to their ultimate destination, cisplatin and related compounds are exposed to a variety of competing ligands, in particular N- and S-donor residues in proteins and peptides [7-9]. Protein binding is related to the occurrence of drug resistance and toxic effects. It is then useful to acquire detailed information about cisplatin reactivity with biological ligands. To this end, small molecules have been selected to mimic biological targets. In a parallel line of investigation, intrinsic properties of cisplatin binding to DNA have been addressed by characterizing cisplatin complexes with ligands of increasing complexity, namely nucleobases and nucleotides, by vibrational ion spectroscopy [40-42]. Similarly, here we first allow simple biomolecules (L) to react with cisplatin forming *cis*-$[PtCl(NH_3)_2(L)]^+$ complexes, to proceed later by considering intact amino acids as entering ligands. Selected ligands are pyridine (Py), 4(5)-methylimidazole (MI), thioanisole (TA), trimethylphosphate (TMP), acetamide (ACM), dimethylacetamide (DMA), urea (U) and thiourea (SU)[43-44]. They either possess a representative functional group (for example the aza group, present in pyridine, is a platination site in DNA) or play themselves a biological role (such as thiourea, used as “rescue agent” to inhibit Pt coordination to S-donor proteins). The formation of a ligand substitution product occurs readily upon mixing an aqueous cisplatin solution with an L solution (Equation 1).

$$cis\text{-}[PtCl(NH_3)_2(H_2O)]^+ + L \rightarrow cis\text{-}[PtCl(NH_3)_2(L)]^+ + H_2O \qquad (1)$$

In view of the stereoretentive character of the substitution reaction, *cis*-$[PtCl(NH_3)_2(L)]^+$ complexes are formed, whose structure can however be interrogated by IRMPD spectroscopy. As an example, Fig. 3 shows the IRMPD spectrum of the *cis*-$[PtCl(NH_3)_2(U)]^+$ complex, which is well accounted for by the calculated IR spectrum of the lowest energy isomer **U_1** [44]. Metal binding is thus verified to engage the carbonyl oxygen rather than an amido nitrogen. Figure 4 presents the IRMPD spectra of the sampled *cis*-$[PtCl(NH_3)_2(L)]^+$ complexes together with their structure assigned on the basis of the agreement between calculated and experimental vibrational spectra. With regard to reactivity, while it is difficult to extract relative data about reaction 1 in solution, gas phase kinetics are amenable to FT ICR MS when the neutral L is volatile enough to ensure a controlled pressure in the cell of the instrument. It was thus possible to observe a trend in bimolecular rate constants following the order TMP > TA > Py [43]. While the aza group

of pyridine and the thiomethyl group of TA are known to be efficient nucleophiles with platinum(II) complexes [10], the high reactivity of TMP, an O-ligand, is somewhat unexpected and suggests a kinetic role for the phosphate groups of nucleotides [45]. It may be underlined once again that this approach, combining ESI MS with IRMPD spectroscopy, provides a unique avenue to characterize the structure of the complex formed in solution. However, for each individual ion, the possibility of rearrangements occurring in the transfer to the gas phase or within the gaseous species needs to be carefully considered.

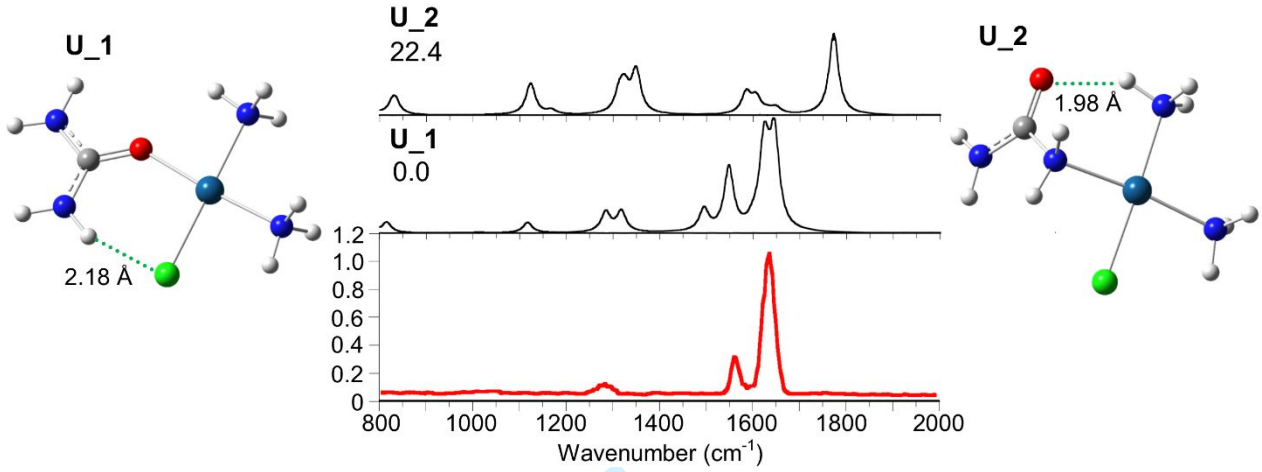

Fig. 3. IRMPD spectrum of *cis*-$[PtCl(NH_3)_2(Urea)]^+$ (red profile) compared with calculated harmonic IR spectra of **U_1** and **U_2** isomers optimized at the B3LYP/6-311+G(d,p) (Pt = LANL2TZ) level (black profiles). Relative free energy at 298 K, in kJ mol^{-1}, is given under each **U_1/2** label. Theoretical spectra are scaled by a 0.974 factor.

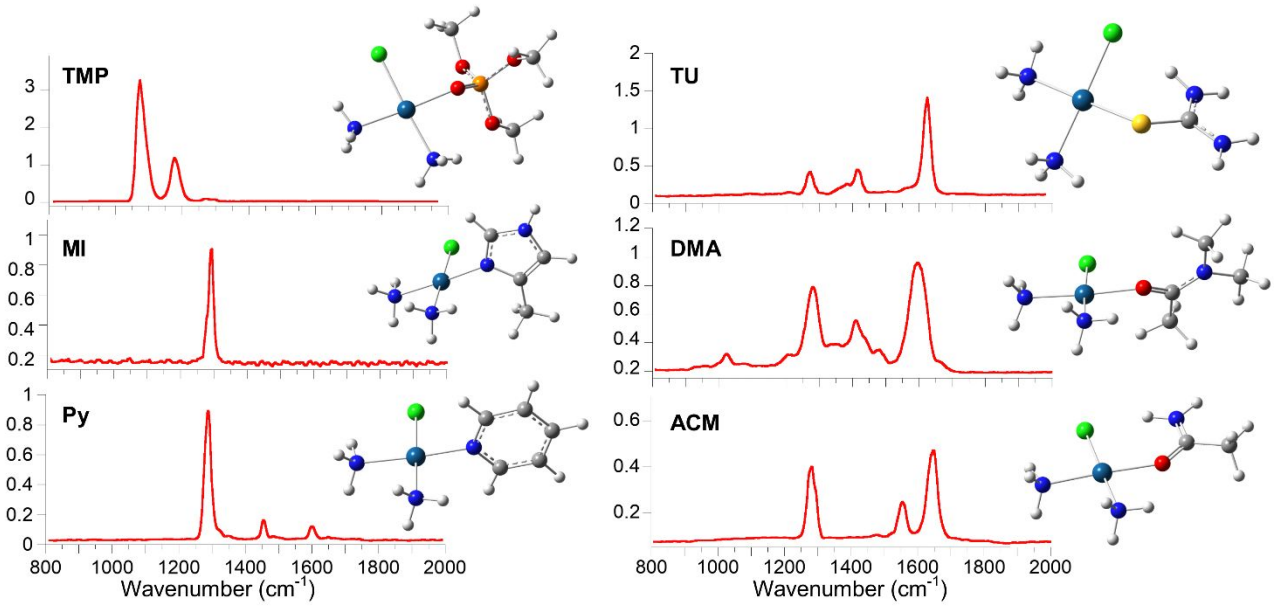

Fig. 4. IRMPD spectra of *cis*-$[PtCl(NH_3)_2(L)]^+$ complexes. Also shown are the structures assigned on the basis of the matching between IRMPD spectra and IR spectra of the optimized geometries at B3LYP/6-311+G(d,p) (Pt = Lanl2TZ) level of theory.

Cisplatin binding to an N-donor amino acid, histidine

The imidazole side group of histidine residues is a favored platination site as shown by several ESI MS and X-ray diffraction studies [8,46-48]. However, cisplating binding to a single L-histidine (His) molecule yields already a complex product pattern, depending on pH and evolving to multiply substituted and chelate complexes, so that the early primary complex deriving from reaction 1 (L = His) is not evidenced [49-50]. Favorably, the *cis*-$[PtCl(NH_3)_2(His)]^+$ complex is clearly identified in ESI MS, as shown in the spectrum reported in Fig. 5 [51]. The primary complex involving the cisplatin adduct where histidine has replaced a chlorido ligand corresponds to the isotopic cluster at *m/z* 418 (*m/z* of the first significant peak in the cluster is henceforth reported). The *cis*-$[PtCl(NH_3)_2(His)]^+$ species of interest may thus be examined for spectroscopic and reactivity properties to obtain structural information [51]. The ions at *m/z* 418 were sampled by collision induced dissociation (CID) at variable energy showing contrasting behavior. While at minimal collision energy already a considerable fraction of ions has undergone loss of NH_3, a sizeable portion is instead resistant to fragmentation even at high collision energy. This behavior suggests the presence of isomeric ions and in fact two families of isomers can be expected depending on the site of Pt binding. Fig. 6 displays the optimized structure of two regioisomers whereby platinum is ligated to an imidazole nitrogen being either N_π (pros, near) or N_τ (tele, far), in reference to their position relative to the side chain (**N_π_1**, **N_π_2**, **N_τ_1**, and **N_τ_2** are the most stable conformers).

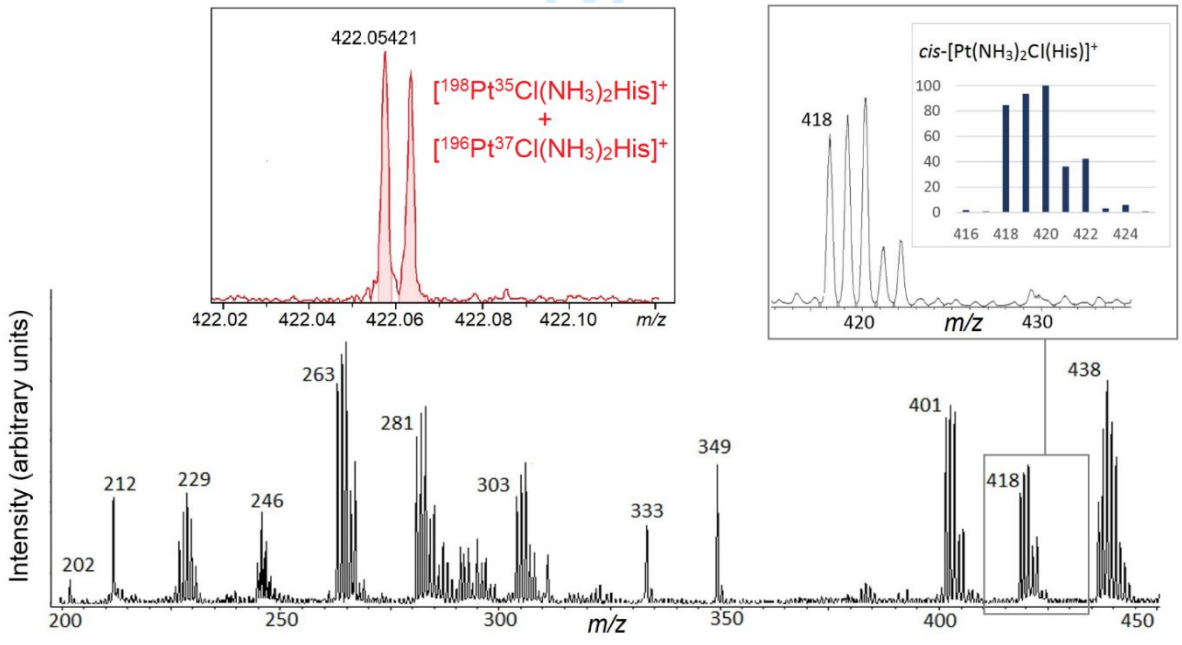

Fig. 5: Mass spectrum of a solution of cisplatin and His (1:1) 5×10^{-5} M in 50:50 methanol/water. The species of interest, the *cis*-$[PtCl(NH_3)_2His]^+$ complex, corresponds to the cluster at *m/z* 418. The assignment is consistent with the isotopic pattern enlarged in the inset, matching the calculated distribution (blue sticks) congruent with the presence of one platinum and one chlorine atom. High resolution FT-ICR mass spectra (an excerpt shown on the upper left panel) confirm the elemental composition.

The presence of both N_π and N_τ isomers explains the fragmentation behavior upon CID because only the N_π geometry may lead by NH_3 loss to a chelate complex where the metal is additionally bound to the amino N atom (N_a) ($[PtCl(NH_3)His(N_\pi,N_a)]^+$), the chelation motif also observed in aqueous solution [49]. Figure 6 displays also the computed IR spectra for **N_π_1**, **N_π_2**, **N_τ_1**, and **N_τ_2** which are compared with the experimental IRMPD spectrum to gain insight into the composition of the sampled ion population. The IRMPD spectrum shows that indeed an ion mixture is present, because none of the IR spectra matches alone the experimental features. The most informative part of the spectrum is the higher energy range where the prominent band at 3497 cm^{-1} is due to the NH stretching mode of the imidazole group which characterizes the IR spectra of **N_π** conformers. In the **N_τ** configuration the imidazole NH is engaged in hydrogen bonding, causing a red shift in the NH stretching frequency. The band at 3565 cm^{-1} arises from the OH stretching mode of a 'free' hydroxyl group, as verified in **N_π_2**, **N_τ_1** and **N_τ_2** isomers. These frequencies are isomer/conformer specific and thus lend themselves to be used for photofragmentation kinetics to probe the composition of the ion mixture [52].

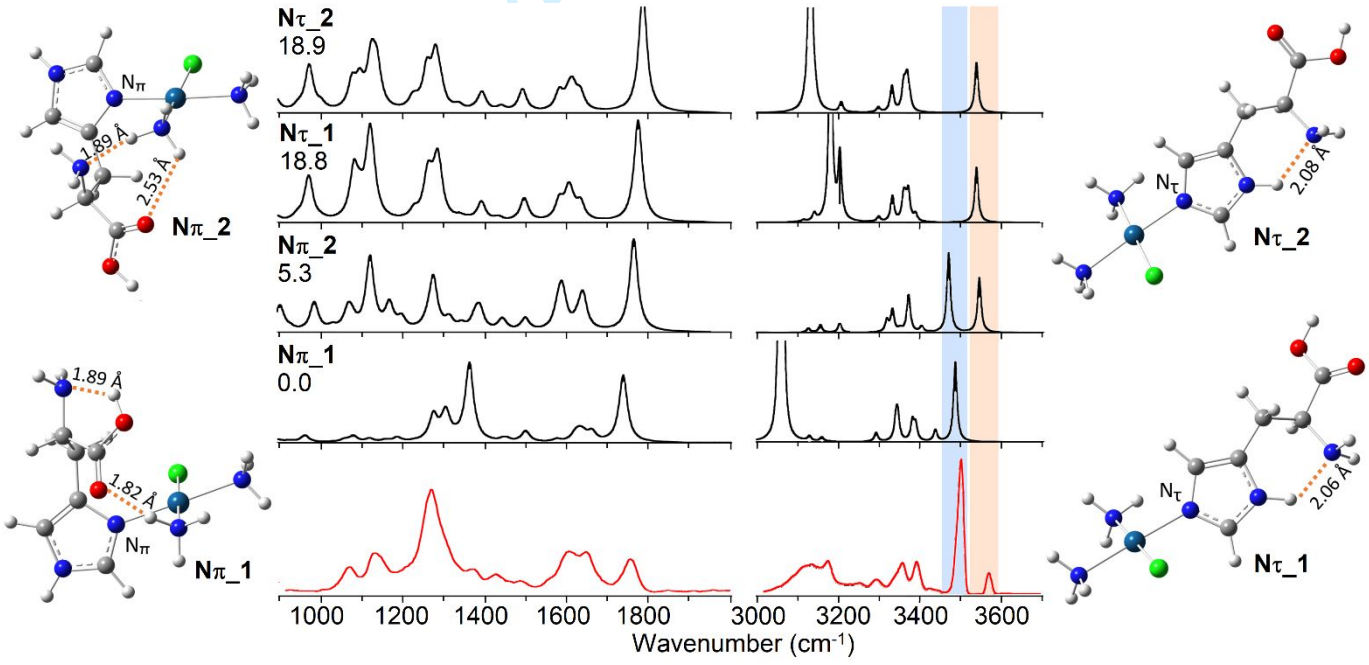

Fig. 6: IRMPD spectrum of *cis*-$[PtCl(NH_3)_2His]^+$ (red profile) compared to the unscaled linear anharmonic IR spectra calculated at B3LYP/6-311+G(d,p) (Pt = LANL2TZ) level for the most stable conformers of N_π and N_τ families of isomers (black profiles). Optimized geometries at the same level of theory are reported together with relative free energies at 298 K in kJ mol^{-1} calculated at the ωB97X-D/6-311+G(d,p) level.

IRMPD kinetics monitored at 3497 and 3565 cm^{-1} are shown in Fig. 7 reporting the decay of the parent ion *cis*-$[PtCl(NH_3)_2His]^+$ abundance as a function of irradiation time. For both kinetics a neat exponential decay is observed with rate constants differing by less than a factor of 2. This behavior is consistent with the presence of **N_π_1** and **N_π_2** conformers, endowed with comparable photofragmentation properties in the two resonances. The photofragmentation kinetics do not proceed to completion and an unreactive fraction is measured equal to 25% and 70% at 3497 and 3565 cm^{-1}, respectively. This finding is accounted for by

N_π_1 not being IR active at 3565 cm^{-1}, while the residual intact fraction at 3497 cm^{-1} is associated to **N_τ** conformers, displaying red-shifted imidazole NH stretch. However, the predicted red shift does not simply account by itself for the missing photofragmentation activity. In fact, this 25% residual intact fraction is also confirmed on other tested absorption frequencies that are commonly active for all **N_π/N_τ** isomers (for example at 3350 and 3392 cm^{-1}). This finding suggests that laser fluence in this frequency range is not adequate to activate **N_τ** species towards NH_3 cleavage, being the process relatively more unfavorable with respect to fragmentation from **N_π** complexes. NH_3 cleavage from **N_π** complexes may be assisted by the amino acid NH_2 group thus forming a chelate complex, a documented process in the platination of histidine in water solution [50]. This intramolecular ligand exchange process is prohibited by the geometry of **N_τ** complexes which yield an energetically high lying three coordinate complex upon release of NH_3. The inference is that the low fluence of the OPO/OPA laser used in this wavenumber range is inadequate to activate IRMPD of **N_τ** isomers. Thus, analysis of the collected data point out that **N_π_1**, **N_π_2**, and **N_τ_1 /N_τ_2** species are present in 45:30:25 ratio in the sampled mixture.

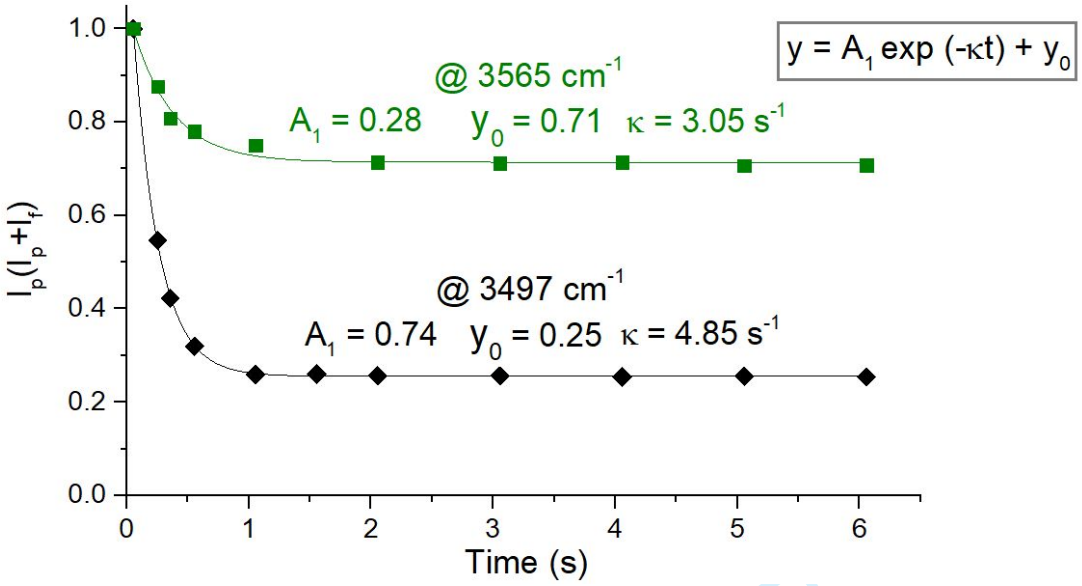

Fig. 7: Plot showing the decay of the parent ion *cis*-$[PtCl(NH_3)_2His]^+$ abundance as a function of irradiation time at two different wavenumbers. Fitting exponential functions are reported.

To summarize, in contrast with a previous report [53], ESI MS has successfully yielded *cis*-$[PtCl(NH_3)_2His]^+$ complexes, namely the primary species deriving from His binding to cisplatin or its monoaqua derivative. IRMPD spectroscopy has revealed a mixture of isomers formed by metal binding to either N_π or N_τ nitrogen of the imidazole side group. The relative fraction of N_π versus N_τ attack could be estimated by the amplitude of photofragmentation processes recorded on diagnostic resonances.

Cisplatin (and transplatin) binding to an S-donor amino acid, methionine

According to hard soft acid base (HSAB) theory, cisplatin, bearing a soft metal is predicted to have high affinity for sulfur containing ligands and in fact sulfur containing peptides and proteins are known to efficiently bind, performing also a transport role for the drug [9, 54-56]. When cisplatin is allowed to react

with methionine (Met), a complex product pattern is observed including both monofunctional and chelate species but, as in the case of His, the early complex displaying the first metal coordination event has not yet been characterized in solution. ESI has once again been used to deliver the ion of interest, $[PtCl(NH_3)_2Met]^+$ at *m/z* 412, formed by reaction of either cisplatin or transplatin, to be assayed for structural characterization [57]. However, typically informative tools in MS, such as CID mass spectra or methods based on ion mobility separation, discriminating ions according to different shape (collision cross section in a bath gas), do not make appreciable distinction between *cis*- and *trans*-$[PtCl(NH_3)_2Met]^+$. Vibrational ion spectroscopy provides the sought solution to the problem [57]. IRMPD spectra reported in Fig. 8 are clearly different for the two isomers, presenting several bands at closely similar frequency, though largely varying in intensity. One may notice, for example, a major band at 1130 cm^{-1} in the spectrum of the trans isomer which corresponds to an only weak one in the spectrum of the cis isomer, while an intense band for the cis complex at 1376 cm^{-1} has a weak counterpart for the trans at ca. 1367 cm^{-1}. However, in order to obtain thorough structural insight, as usual, one needs to explore potential geometries for the two isomers which best account for the recorded spectra.

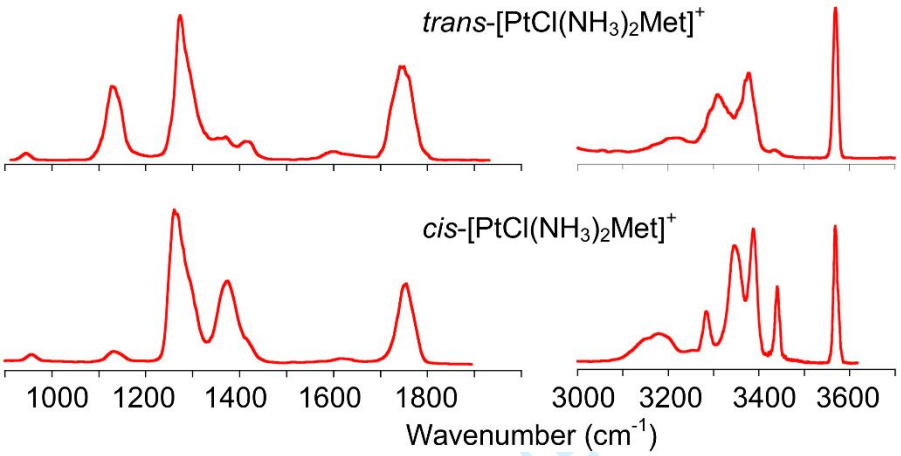

Fig. 8: IRMPD spectra of *cis*-$[PtCl(NH_3)_2Met]^+$ and *trans*-$[PtCl(NH_3)_2Met]^+$ complexes.

The most stable isomers for *cis*-$PtCl(NH_3)_2Met]^+$ complexes are presented in Fig. 9 together with the associated IR spectra. S-ligated complexes, **cS1** and **cS2** at 0 and 4 kJ/mol relative free energy, are more stable than N-ligated species, for example **cN1** at 18 kJ/mol.

Comparing the computed IR spectra with the experimental IRMPD spectrum suggests that the contribution of more than one geometry though a mixture of **cS1** and **cS2** may well explain the observed features. In particular, in the higher wavenumber range, **cS2** may be attributed the OH stretching band at 3564 cm^{-1}, due to the 'free' OH of the carboxylic group in syn configuration. The anti carboxylic group in **cS1** allows OH···NH_2 hydrogen bonding which causes the calculated O-H stretching to be shifted at 3083 cm^{-1}. However, a characteristic mode revealing the ligation motif is the asymmetric stretching of the α-amino group. This mode is responsible for the IRMPD band at 3443 cm^{-1}, corresponding to the calculated resonance appearing in the spectra of **cS** isomers. In contrast, IR activity is missing in the spectra of **cN** isomers at this frequency because platination at the NH_2 group as in **cN1** shifts the asymmetric NH_2 stretching to 3318 cm^{-1}. It may be noted that in both **cS1** and **cS2** isomers the NH_2 group is involved in hydrogen bonding, the already cited OH···NH_2 interaction in **cS1** and HNH···O=C in **cS2** isomers, apparently affecting the asymmetric stretching wavenumber to a comparable extent.

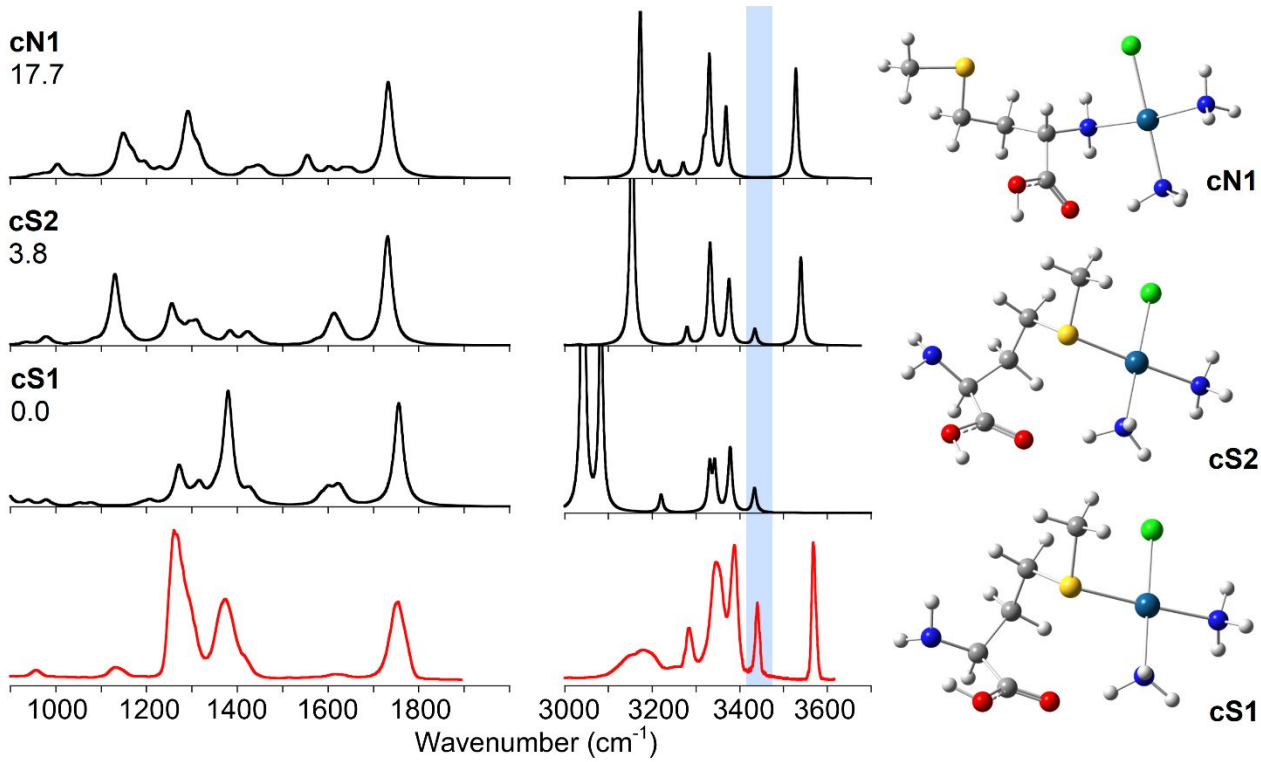

Fig. 9: IRMPD spectrum of *cis*-[PtCl(NH_3)$_2$Met]$^+$ (red profile), compared with calculated unscaled anharmonic spectra of selected isomers at the B3LYP/6-311++G(2df,pd) level using the 6-311++G(3df) basis set for S and the pseudopotential LANL2TZ-f for Pt. The corresponding optimized geometries are shown on the right. Relative free energies at 298 K in kJ mol^{-1} are reported.

trans-PtCl(NH_3)$_2$Met]$^+$ complexes present S- and N-ligated complexes that are more closely distributed in relative energy. Fig. 10 displays the lower lying conformers **tN1**, **tS1** and **tS2**, collectively contributing to the recorded IRMPD spectrum. In this spectrum the band at 3434 cm^{-1}, recognized to pertain to the asymmetric stretching of the α-amino group and as such appearing as a major feature in the IR spectra of **tS1** and **tS2**, is noticeably weaker when compared with the corresponding one in the spectrum of the cis isomer. This evidence and the similar energy of **tS** and **tN** isomers support a comparable contribution of the two families of complexes in the sampled ions. However, a semiquantitative evaluation is afforded by photofragmentation kinetics at the diagnostic NH_2 asymmetric stretching at 3443/3434 cm^{-1} in the IRMPD spectra of *cis*- and *trans*-[PtCl(NH_3)$_2$Met]$^+$ complexes, respectively.

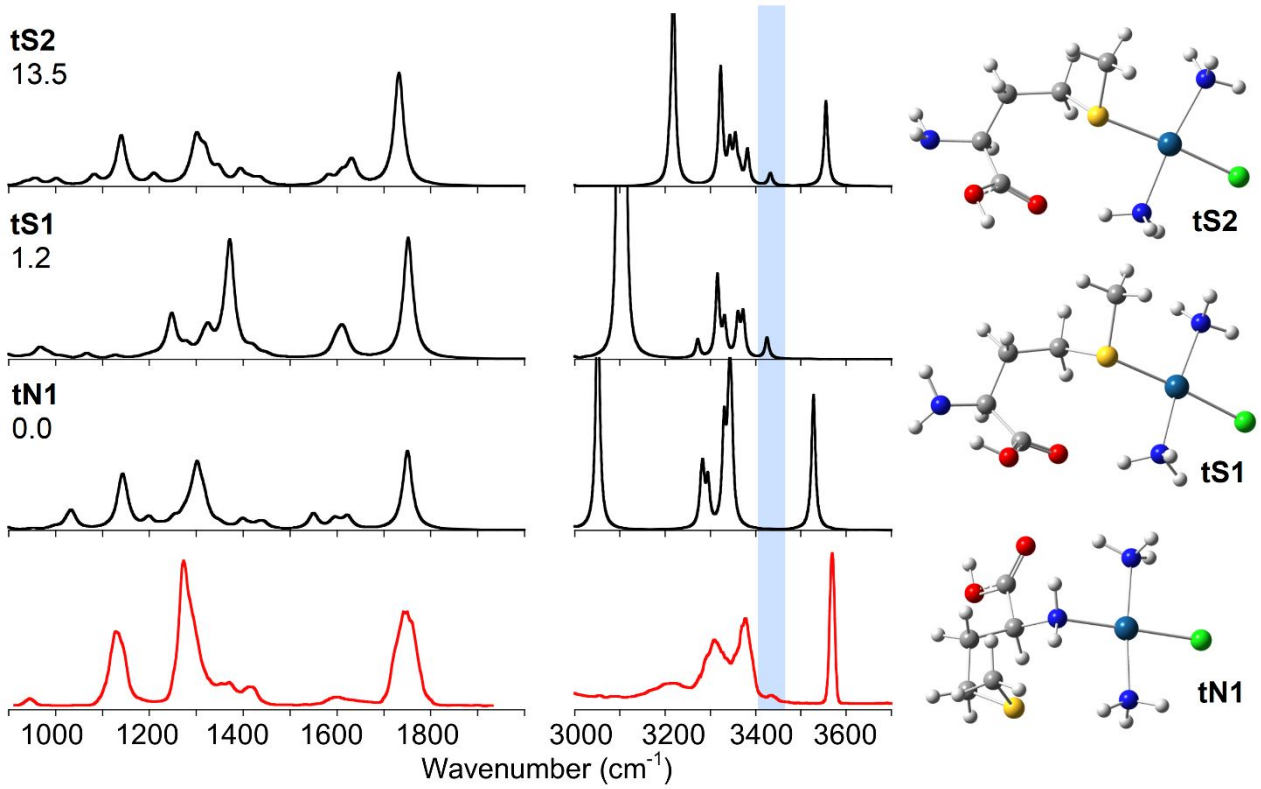

Fig. 10: IRMPD spectrum of *trans*-[PtCl(NH_3)$_2$Met]$^+$ (red profile), compared with calculated unscaled anharmonic spectra of selected isomers at the B3LYP/6-311++G(2df,pd) level using the 6-311++G(3df) basis set for S and the pseudopotential LANL2TZ-f for Pt. The corresponding optimized geometries are shown on the right. Relative free energies at 298 K in kJ mol^{-1} are reported.

The exponential plots reported in Fig. 11 do not differ significantly in terms of time constant but considerably more in the amplitude of the process. In fact, the photofragmentation leaves an unreactive fraction of *trans*-isomer of ca. 64% while the process goes almost to completion for *cis*-[PtCl(NH_3)$_2$Met]$^+$. It may be thus inferred that cisplatin preferentially reacts at the thiomethyl group whereas transplatin is less selective yielding also N-coordination. A rationale for the different behavior may be ascribed to the trans influence in square planar platinum(II) complexes. In fact, in the case of transplatin, S-platination leads to a complex whereby two donating groups with rather high trans influence (thiomethyl and chloride) are placed in trans relationship to each other, competing for donation and destabilizing the complex [12,39,58]. Under these circumstances, the typically favored S-attack becomes relatively disfavored.

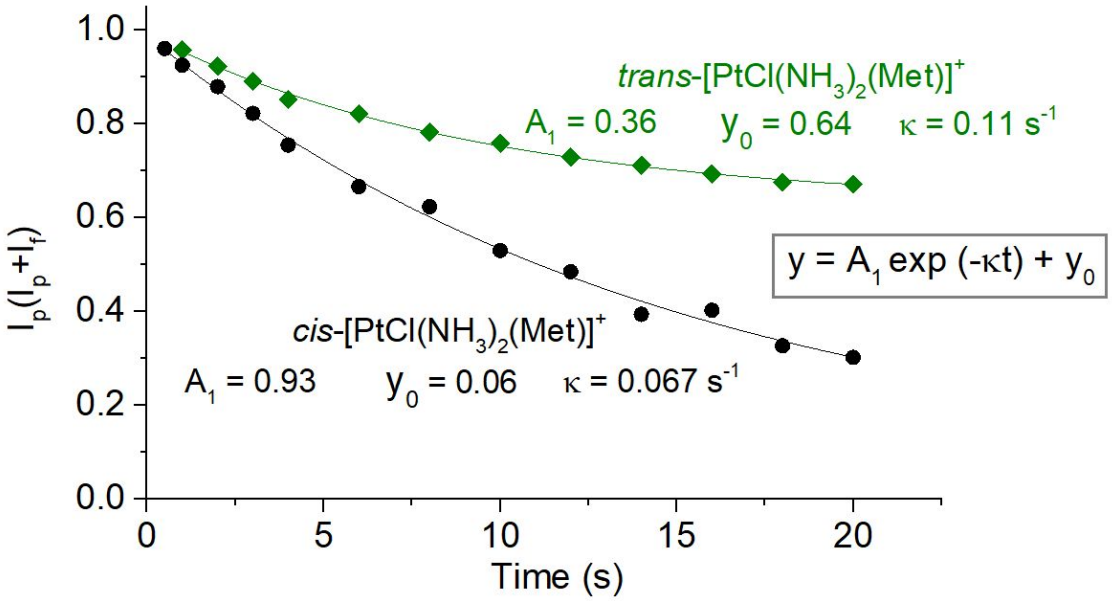

Fig. 11: Plots showing the decay of the relative abundancies of the sampled ions, *cis*- and *trans*-[PtCl(NH$_3$)$_2$Met]$^+$, as a function of the irradiation time. Fitting exponential functions are reported.

Conclusions

Electrospray ionization coupled to mass spectrometry and IR laser spectroscopy combined with quantum chemical calculations have released structural insight on the early complexes involved in the biological fate of cisplatin or on simple models thereof. The initial active species are obtained by an aquation process replacing the chlorido ligand(s) and IRMPD spectroscopy has revealed the vibrational features of *cis*- and *trans*-[PtX(NH$_3$)$_2$(H$_2$O)]$^+$ (X = Cl, OH) complexes. Cisplatin undergoes ligand substitution with simple molecules mimicking biological targets in aqueous solution yielding, *cis*-[PtCl(NH$_3$)$_2$L]$^+$ (X = Py, MeIm, TA, TMP, ACM, DMA, U, and SU) complexes. These complexes, assayed by IRMPD spectroscopy, have shown regioselective platination in the presence of potentially competing sites (for example the carbonyl oxygen of U or the phosphoryl oxygen of TMP). Histidine and methionine (together with cysteine) residues are the main Pt anchoring sites within peptides and proteins. IRMPD spectroscopy and photofragmentation kinetics have allowed us to obtain a detailed cisplatin coordination pattern yielding information on both binding regioselectivity and also on the most favored conformers in each family of isomers (for example within N_π and N_τ isomers in His complexes). It may be underlined that the observed binding motifs of cisplatin with the sampled bioligands concern substitution products formed in aqueous solution and sampled in the gas phase. Indeed, any isomerization involving breaking and rearrangement of coordination bonds to the metal is inhibited by high activation energies in the gaseous isolated species [51,57]. However, the reaction with the free sampled amino acids may bear consequence on the platination of proteins in biological media. In fact, according to reported X-ray diffraction studies and MS investigations, Pt binding involves mainly solvent exposed protein side chains [7,55]. The present contribution may thus provide a useful reference for the plain early platination event occurring in the aqueous medium from where the sampled ionic complexes are extracted and isolated.

Acknowledgments: This research was supported by the Università degli Studi di Roma La Sapienza and by the European Commission (CLIO project IC14-011).
The authors are grateful to Philippe Maitre, Jean-Michel Ortega, Debora Scuderi, Vincent Steinmetz and the CLIO team and to Annito Di Marzio for experiments at the OPO/OPA laser.

REFERENCES

[1] B. Rosenberg, L. V. Camp, J. E. Trosko, V. H. Mansour. *Nature* **222**,385 (1969).
[2] R. A. Alderden, M. D. Hall, T. W. Hambley. *J. Chem. Ed.* **83**, 728 (2006).
[3] D. Wang, S. J.Lippard. *Nat. Rev. Drug Discov.* **4**, 307 (2005).
[4] J. Kozelka, F. Legendre, F. Reeder, J.-C. Chottard. *Coord. Chem. Rev.* **190-192**, 61 (1999).
[5] A. V. Klein, T. W. Hambley. *Chem. Rev.* **109**, 4911 (2009).
[6] B. Lippert. *Cisplatin: Chemistry and Biochemistry of a Leading Anticancer Drug*, Wiley-VCH, Zurich, Switzerland (1999).
[7] A. Merlino, T. Marzo, L. Messori. *Chem. Eur. J.* **23**, 6942 (2017).
[8] A. Casini, J. Reedijk. *Chem. Sci.* **3**, 3135 (2012).
[9] H. Li, Huilin,Y. Zhao, H. I. A. Phillips, Y. Qi, T.-Y Lin, P. J. Sadler, P. B. O'Connor. *Anal. Chem.* **83**, 5369 (2011).
[10] Z. D. Bugarcic, J. Bogojeski, B. Petrovic, S. Hochreuther, R. van Eldik. *Dalton Trans.* **41**, 12329 (2012).
[11] D. V. Deubel. *J. Am. Chem. Soc.* **126**, 5999 (2004).
[12] D. T. Richens. *Chem. Rev.* **105**, 1961 (2005).
[13] S. J. Berners-Price, T. G. Appleton. *The chemistry of cisplatin in aqueous solution.* In *Platinum-based drugs in cancer therapy. Cancer drug discovery and development* (L. R. Kelland, N. P. Farrell eds.), pp. 3-35. Humana Press, Totowa, NJ (2000).
[14] J. Vinje, E. Sletten, J. Kozelka. *Chem. Eur. J.* **11**, 3863 (2005).
[15] S. J. Lippard. *Science* **218**, 1075 (1982).
[16] S. Hochreuther, R. Puchta, R. van Eldik. *Inorg. Chem*. **50**, 12747 (2011).
[17] Z. Xu, J. S. Brodbelt. *J. Am. Soc. Mass Spectrom.* **25**, 71 (2014).
[18] L. A. Hammad, G. Gerdes, P. Chen. *Organometallics* **24**, 1907 (2005).
[19]M. Cui, L. Ding, Z. Mester. *Anal. Chem*. **75**, 5847 (2003).
[20] M. L. Styles, R. A. J. O'Hair, W. D. McFadyen, L. Tannous, R. J. Holmes, R. W. Gable. *J. Chem. Soc., Dalton Trans.* **0**, 93 (2000).
[21] J. Oomens, B. G. Sartakov, G. Meijer, G. von Helden. *Int. J. Mass Spectrom.* **254**, 1 (2006).
[22] L. MacAleese, P. Maitre. *Mass Spectrom. Rev.* **26**, 583 (2007).
[23] L. Jašíková, J. Roithová. *Chem. Eur. J.* **24**, 3374 (2018).
[24] T. D. Fridgen. *Mass Spectrom. Rev.* **28**, 586 (2009).
[25] J. R. Eyler. *Mass Spectrom. Rev.* **28**, 448 (2009).
[26] N. C. Polfer, J. Oomens. *Mass Spectrom. Rev.* **28**, 468 (2009).
[27] N. C. Polfer. *Chem. Soc. Rev.* **40**, 2211 (2011).
[28] M. Katari, E. Payen de la Garanderie, E. Nicol, V. Steinmetz, G. van der Rest, D. Carmichael, G. Frison. *Phys. Chem. Chem. Phys.* **17**, 25689 (2015).
[29] B. Chiavarino, M. E. Crestoni, S. Fornarini, S. Taioli, I. Mancini, P. Tosi. *J. Chem. Phys.* **137**, 024307 (2012).
[30] A. Ciavardini, A. Dalla Cort, S. Fornarini, D. Scuderi, A. Giardini, G. Forte, E. Bodo, S. Piccirillo. *J. Mol. Spectrosc.* **335**, 108 (2017).
[31] R. C. Dunbar, J. Martens, G. Berden, J. Oomens. *Int. J. Mass Spectrom.* **429**, 198 (2018).
[32] A. M. Chalifoux, G. C. Boles, G. Berden, J. Oomens, P. B. Armentrout. *Phys. Chem. Chem. Phys.* **20**, 20712 (2018).
[33] K. Peckelsen, J. Martens, G. Berden, J. Oomens, R. C.Dunbar, A. J.H.M.Meijer, M.Schäfer. *J. Mol. Spectrosc.* **332**, 38 (2017).
[34] B. E. Ziegler, R. A. Marta, M. B. Burt, T. B. McMahon. *Inorg. Chem.* **53**, 2349 (2014).

[35] T. E. Hofstetter, C. Howder, G. Berden, J. Oomens, P. B. Armentrout. *J. Phys. Chem. B* **115**, 12648 (2011).
[36] A. De Petris, A. Ciavardini, C. Coletti, N. Re, B. Chiavarino, M. E. Crestoni, S. Fornarini. *J. Phys. Chem. Lett.* **4**, 3631 (2013).
[37] D. Corinti, C. Coletti, N. Re, S. Piccirillo, M. Giampà, M. E. Crestoni, S. Fornarini. *RSC Adv.* **7**, 15877 (2017).
[38] C. C. He, B. Kimutai, X. Bao, L. Hamlow, Y. Zhu, S. F. Strobehn, J. Gao, G. Berden, J. Oomens, C. S. Chow, M. T. Rodgers. *J. Phys. Chem. A* **119**, 10980 (2015).
[39] Z.Chval, M. Sip, J. V. Burda. *J. Comput. Chem.* **29**, 2370 (2008).
[40] B. Chiavarino, M. E. Crestoni, S. Fornarini, D. Scuderi, J.-Y. Salpin. *Inorg. Chem.* **56**, 8793 (2017).
[41] B. Chiavarino, M. E. Crestoni, S. Fornarini, D. Scuderi, J.-Y. Salpin. *Inorg. Chem.* **54**, 3513 (2015).
[42] B. Chiavarino, M. E. Crestoni, S. Fornarini, D. Scuderi, J.-Y. Salpin. *J. Am. Chem. Soc.* **135**, 1445 (2013).
[43] D. Corinti, C. Coletti, N. Re, B. Chiavarino, M. E. Crestoni, S. Fornarini. *Chem. Eur. J.* **22**, 3794 (2016).
[44] D. Corinti, C. Coletti, N. Re, R. Paciotti, P. Maitre, B. Chiavarino, M. E. Crestoni, S. Fornarini. *Int. J.Mass Spectrom.* **435**, 7 (2019).
[45] M. S. Davies, S. J. Berners-Price, T. W. Hambley. *Inorg. Chem.* **39**, 5603 (2000).
[46] V. Calderone, A. Casini, S. Mangani, L. Messori, P. L. Orioli. *Angew. Chem.* **45**, 1267 (2006).
[47] H. Li, Y. Zhao, H. I. A. Phillips, Y. Qi, T.-Y. Lin, P. J. Sadler, P. B. O'Connor. *Anal. Chem.* **83**, 5369 (2011).
[48] A. Casini, A. Guerri, C. Gabbiani, L. Messori. *J. Inorg. Biochem.* **102**, 995 (2008).
[49] V. Saudek, H. Pivcova, D. Noskova, J. Drobnik. *J. Inorg. Biochem.* **23**, 55 (1985).
[50] T. G. Appleton. *Coord. Chem. Rev.* **166**, 313 (1997).
[51] D. Corinti, A. De Petris, C. Coletti, N. Re, B. Chiavarino, M. E. Crestoni, S. Fornarini. *ChemPhysChem* **18**, 318 (2017).
[52] J. S. Prell, T. M. Chang, J. A. Biles, G. Berden, J. Oomens, E. R. Williams. *J. Phys. Chem. A* **115**, 2745 (2011).
[53] H. Liu, N. Zhang, M. Cui, Z. Liu, S. Liu. *Int. J. Mass Spectrom.* **409**, 59 (2016).
[54] J. Reedijk. *Chem. Rev.* **99**, 2499 (1999).
[55] L. Messori, A. Merlino. *Coord. Chem. Rev.* **315**, 67 (2016).
[56] C. M. Sze, G. N. Khairallah, Z. Xiao, P. S. Donnelly, R. A. J. O'Hair and A. G. J. Wedd, *J. Biol. Inorg. Chem.*, **14**, 163 (2009).
[57] R. Paciotti, D. Corinti, A. De Petris, A. Ciavardini, S. Piccirillo, C. Coletti, N. Re, P. Maitre, B. Bellina, P. Barran, B. Chiavarino, M. E. Crestoni, S. Fornarini. *Phys.Chem. Chem. Phys.* **19**, 26697 (2017).
[58] B. Pinter, V. Van Speybroeck, M. Waroquier, P. Geerlings, F. De Proft. *Phys. Chem. Chem. Phys.* **15**, 17354 (2013).

Davide Corinti, Roberto Paciotti, Nazzareno Re, Cecilia Coletti, Barbara Chiavarino, Maria Elisa Crestoni and Simonetta Fornarini*

Binding motifs of cisplatin interaction with simple biomolecules and aminoacid targets probed by IR ion spectroscopy

Davide Corinti, Barbara Chiavarino, Maria Elisa Crestoni and Simonetta Fornarini: Dipartimento di Chimica e Tecnologie del Farmaco, Università degli Studi di Roma La Sapienza, P.le A. Moro 5, I-00185 Roma, Italy
E-mail: simonetta.fornarini@uniroma1.it

Roberto Paciotti, Nazzareno Re, Cecilia Coletti: Dipartimento di Farmacia
Università G. D'Annunzio Chieti-Pescara, Via dei Vestini 31, I-66100 Chieti, Italy

Abstract: The primary intermediates resulting from the interaction of cisplatin, *cis*-($PtCl_2(NH_3)_2$], most widespread antitumor drug, with biomolecular targets are characterized. Electrospray ionization is used to deliver ions formed in solution into the gas phase where they are structurally interrogated by vibrational "action" spectroscopy in conjunction with quantum chemical calculations. The aquation products, *cis*-$[PtX(NH_3)_2(H_2O)]^+$ (X = Cl, OH), lying along the path responsible for biological activity, are shown to display distinctive features responding to ligation pattern and optimized geometry. The IR spectra of *trans*-$[PtX(NH_3)_2(H_2O)]^+$ are different, testifying that *cis* and *trans* complexes are stable, non interconverting species both in solution and in the gas phase. Ligand substitution by simple nucleophiles (L = pyridine, 4(5)-methylimidazole, thioanisole, trimethylphosphate, acetamide, dimethylacetamide, urea and thiourea) yields *cis*-$[PtCl(NH_3)_2(L)]^+$ complexes displaying remarkable regioselectivity whenever L presents multiple candidate platination sites. The incipient formation of cisplatin-derived complexes with the recognized biological amino acid targets L-histidine (His) and L-methionine (Met) has been investigated revealing the primary platination event to be mainly directed at the N_π atom of the imidazole side chain of His and to the thiomethyl sulfur of Met. The isomer and conformer population of the ensuing *cis*-$[PtCl(NH_3)_2(Met/His)]^+$ complexes, sampled in the gas phase, can be ascertained by photofragmentation kinetics on isomer/conformer specific resonances.

Keywords: cisplatin, transplatin, IRMPD spectroscopy, photofragmentation kinetics, ligand substitution

Introduction

Cisplatin [*cis*-diamminedichloroplatinum(II), A in Scheme 1] is one of the most widely used chemotherapeutic agents for the treatment of various tumors, a position held since several decades (FDA approval dates back to 1978), following the serendipitous discovery of its anticancer activity by Rosenberg in the 1960s [1-2]. Nowadays cisplatin still represents the reference molecule for a large number of platinum(II) and platinum(IV) compounds, being designed and tested for tumor growth inhibition. Binding

of cisplatin to DNA is ultimately responsible for cell death and occurs via stepwise replacement of chlorido ligands by a solvent assisted mechanism [3-6]. Hydrolysis leads to charged complexes such as *cis*-$[PtCl(NH_3)_2(H_2O)]^+$ and *cis*-$[Pt(OH)(NH_3)_2(H_2O)]^+$, prone to react by electrostatic preassociation and nucleophilic substitution of aqua ligand(s) by nucleobases and final crosslink formation. Besides DNA, cisplatin is known to bind proteins and small molecules such as glutathione through sulfur or nitrogen donor moieties [7-9]. Given the high interest attached to cisplatin reactions with biomolecules, a considerable number of mechanistic studies have been devoted to clarify ligand substitution processes of platinum(II) complexes in protic media. However, the ligand substitution reactivity of platinum(II) complexes in protic solvents is rather driven towards the formation of complex mixtures of various species [10-14]. Polynuclear and chelated complexes are formed, depending on pH, which governs prototropic equilibria [15-16]. Thus, picking a single specific species to be assayed for structure and reactivity behavior is typically not an easy task. This goal has attracted our interest, aiming to gain a comprehensive molecular level description of the interactions of cisplatin with biomolecular targets such natural amino acids or simple models thereof, the focus being on the early event of metal ligand bonding. The use of mass spectrometry (MS) together with electrospray ionization (ESI) presents considerable advantages because it allows to extract charged species, which may otherwise be fleeting intermediates in solution, and isolate them in a highly dilute environment. The present study is based mainly on Fourier transform ion cyclotron resonance (FT-ICR) MS coupled with ESI. ESI is well suited to extract and analyze cisplatin-related complexes formed in aqueous solution [17-20], which are then accumulated and driven to the FT-ICR cell. In this environment, minimizing any perturbing influence, cisplatin complexes may be characterized for their bimolecular reactivity by ion-molecule reactions, for their fragmentation behavior by collision induced dissociation MS, and for their structural features by Infra Red Multiple Photon Dissociation (IRMPD) spectroscopy combined with quantum chemical calculations. Indeed, detailed structural information about gaseous charged species is currently available using this "action" IR spectroscopy, based on the photofragmentation process induced by the non-coherent absorption of IR photons in resonance with active vibrational modes [21-27]. A wide variety of transition metal complexes have already been characterized by IRMPD spectroscopy, such as, for example, metastable reduced zinc complexes [28], copper resveratrol complexes [29], Zn-salophen complexes with chemosensing properties [30], besides various complexes presenting amino acids and peptides bound to transition metals [31-35].

In this report three main issues will be covered: (i) an outline of the developing information about structural and reactivity features of simple cisplatin derived complexes through IRMPD spectroscopy; (ii) bonding motifs from cisplatin interaction with histidine; (iii) bonding motifs from cis- and transplatin interaction with methionine. Transplatin [*trans*-diamminedichloroplatinum(II), B in Scheme 1] is not endowed with anticancer activity, due to its higher reactivity, responsible for side reactions, and to its inability to form 1,2-adducts [2]. It provides a useful reference as alternative isomer, though.

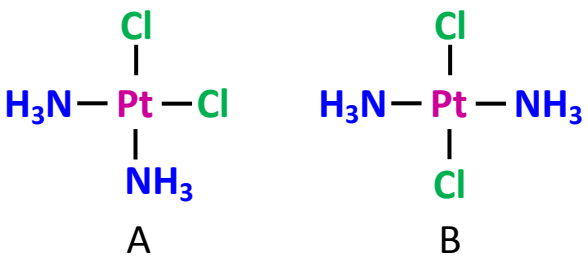

Scheme1: Cisplatin (A) and transplatin (B).

Results and discussion

Cisplatin (and transplatin) aquation and ligand exchange with simple biomolecules

Cisplatin undergoes aquation (replacement of one chlorido ligand with water) in aqueous solution. The controlled hydrolysis, occurring in a suitable time scale preliminarily to DNA binding, is a key step in the antitumor activity. Both singly and diaquated complexes are formed, also the latter believed to contribute to DNA platination which is favored in both cases by the Coulombic interaction of the DNA polyanion with the positively charged complexes. At the same time the charged *cis*-$[PtCl(NH_3)_2(H_2O)]^+$ and *cis*-$[Pt(OH)(NH_3)_2(H_2O)]^+$ complexes are well amenable to ESI-MS analysis allowing them to be characterized by vibrational spectroscopy [36,37]. In their most stable geometry the sampled *cis*-$[PtX(NH_3)_2(H_2O)]^+$ (X = Cl, OH) ions (Fig. 1-2) present the aqua ligand oriented towards X, according to MP2 and DFT calculations. The ensuing hydrogen bonding interaction is responsible for the relatively low frequency of the asymmetric/symmetric OH_2 stretching modes measured experimentally at 3624/3531 and 3600/~~3492~~ 3442 cm^{-1}, for X = Cl and OH, respectively (Fig. 1-2). Incidentally, the evidence obtained by IRMPD experiments needs to be thoroughly examined in parallel with ab initio computations on the candidate species. The selection of the most effective theoretical approach is thus an essential point, as well underlined in the structural determination of a glicine linked cisplatin derivative [38].

Square planar platinum(II) complexes are known to undergo ligand substitution with stereoretention [12]. This notion is confirmed by IRMPD spectroscopy of the aqua complexes formed by hydrolysis of transplatin (Fig. 1-2). In fact, the so-obtained *trans*-$[PtX(NH_3)_2(H_2O)]^+$ (X = Cl, OH) complexes present quite distinct spectra. In particular, the H atoms of the aqua ligand are not engaged in hydrogen bonding which places the asymmetric/symmetric OH_2 stretching modes at 3683/3596 and 3683/3600 cm^{-1}, for X = Cl and OH, respectively. This finding also demonstrates that *cis*-/*trans*-$[PtX(NH_3)_2(H_2O)]^+$ complexes are stable, non interconverting species in the gas phase. Interestingly, the photofragmentation process releases water and the rate of *trans*-$[PtX(NH_3)_2(H_2O)]^+$ isomers is an order of magnitude higher than for the cis counterparts. This result may be viewed as illustration of the trans effect exerted by a trans ligand in labilizing a leaving group departure, which agrees with the order $Cl^- > NH_3$ [2,12,39].

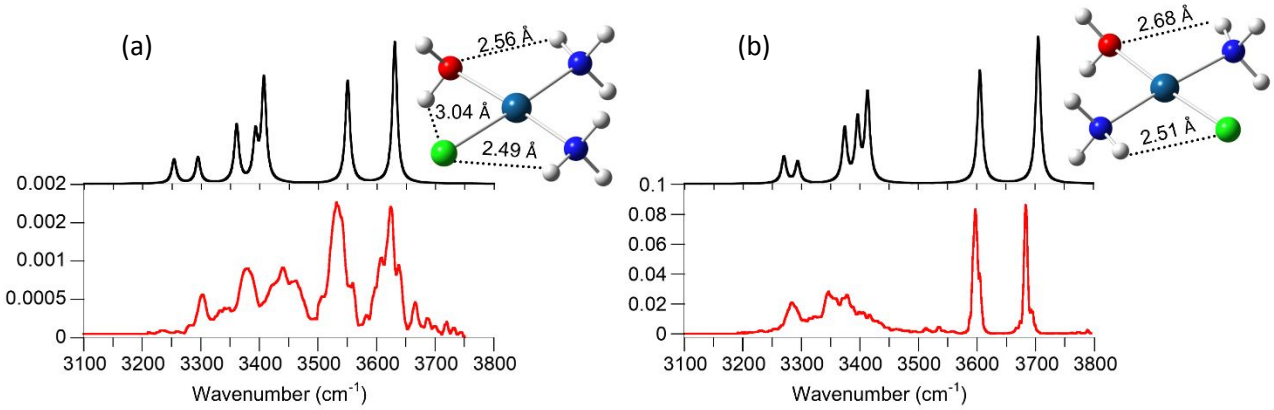

Fig. 1: Experimental IRMPD spectra of *cis*-$[PtCl(NH_3)_2(H_2O)]^+$ (a) and *trans*-$[PtCl(NH_3)_2(H_2O)]^+$ (b) (red profiles) compared with calculated harmonic IR spectra (black profiles) of optimized structures (top right) at MP2/cc-pVTZ (Pt = LANL2TZ) level of theory. Theoretical spectra are scaled by a 0.957 factor.

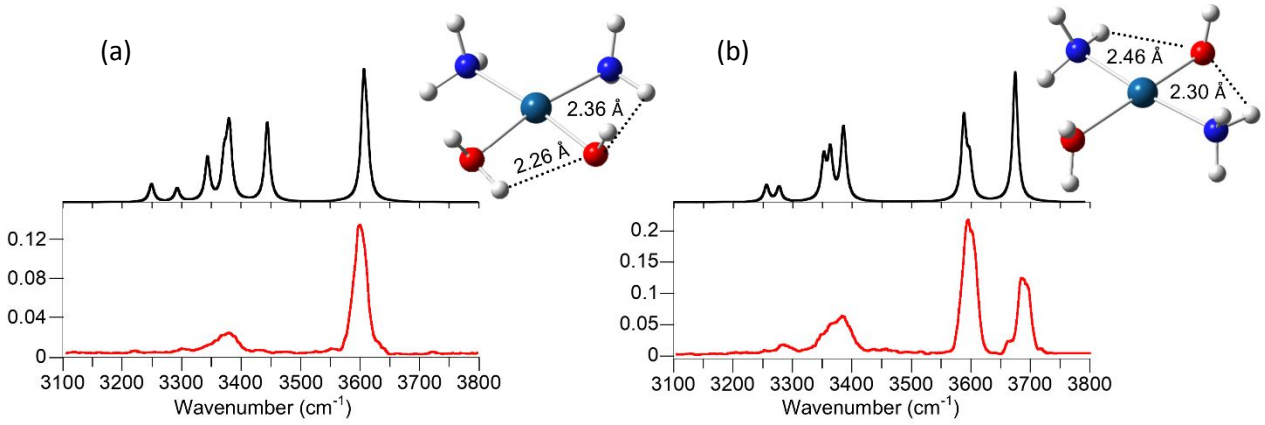

Fig. 2: Experimental IRMPD spectra of *cis*-$[Pt(OH)(NH_3)_2(H_2O)]^+$ (a) and *trans*-$[Pt(OH)(NH_3)_2(H_2O)]^+$ (b) (red profiles) compared with calculated harmonic IR spectra (black profiles) of optimized structures (top right) at B3LYP/cc-pVTZ (Pt = aug-cc-pVTZ-PP) level of theory. Theoretical spectra are scaled by a 0.957 factor.

In the biological environment and along the path to their ultimate destination, cisplatin and related compounds are exposed to a variety of competing ligands, in particular N- and S-donor residues in proteins and peptides [7-9]. Protein binding is related to the occurrence of drug resistance and toxic effects. It is then useful to acquire detailed information about cisplatin reactivity with biological ligands. To this end, small molecules have been selected to mimic biological targets. In a parallel line of investigation, intrinsic properties of cisplatin binding to DNA have been addressed by characterizing cisplatin complexes with ligands of increasing complexity, namely nucleobases and nucleotides, by vibrational ion spectroscopy [40-42]. Similarly, here we first allow simple biomolecules (L) to react with cisplatin forming *cis*-$[PtCl(NH_3)_2(L)]^+$ complexes, to proceed later by considering intact amino acids as entering ligands. Selected ligands are pyridine (Py), 4(5)-methylimidazole (MI), thioanisole (TA), trimethylphosphate (TMP), acetamide (ACM), dimethylacetamide (DMA), urea (U) and thiourea (SU)[43-44]. They either possess a representative functional group (for example the aza group, present in pyridine, is a platination site in DNA) or play themselves a biological role (such as thiourea, used as “rescue agent” to inhibit Pt coordination to S-donor proteins). The formation of a ligand substitution product occurs readily upon mixing an aqueous cisplatin solution with an L solution (Equation 1).

$$cis\text{-}[PtCl(NH_3)_2(H_2O)]^+ + L \rightarrow cis\text{-}[PtCl(NH_3)_2(L)]^+ + H_2O \qquad (1)$$

In view of the stereoretentive character of the substitution reaction, *cis*-$[PtCl(NH_3)_2(L)]^+$ complexes are formed, whose structure can however be interrogated by IRMPD spectroscopy. As an example, Fig. 3 shows the IRMPD spectrum of the *cis*-$[PtCl(NH_3)_2(U)]^+$ complex, which is well accounted for by the calculated IR spectrum of the lowest energy isomer **U_1** [44]. Metal binding is thus verified to engage the carbonyl oxygen rather than an amido nitrogen. Figure 4 presents the IRMPD spectra of the sampled *cis*-$[PtCl(NH_3)_2(L)]^+$ complexes together with their structure assigned on the basis of the agreement between calculated and experimental vibrational spectra. With regard to reactivity, while it is difficult to extract relative data about reaction 1 in solution, gas phase kinetics are amenable to FT ICR MS when the neutral L is volatile enough to ensure a controlled pressure in the cell of the instrument. It was thus possible to observe a trend in bimolecular rate constants following the order TMP > TA > Py [43]. While the aza group

of pyridine and the thiomethyl group of TA are known to be efficient nucleophiles with platinum(II) complexes [10], the high reactivity of TMP, an O-ligand, is somewhat unexpected and suggests a kinetic role for the phosphate groups of nucleotides [45]. It may be underlined once again that this approach, combining ESI MS with IRMPD spectroscopy, provides a unique avenue to characterize the structure of the complex formed in solution. However, for each individual ion, the possibility of rearrangements occurring in the transfer to the gas phase or within the gaseous species needs to be carefully considered.

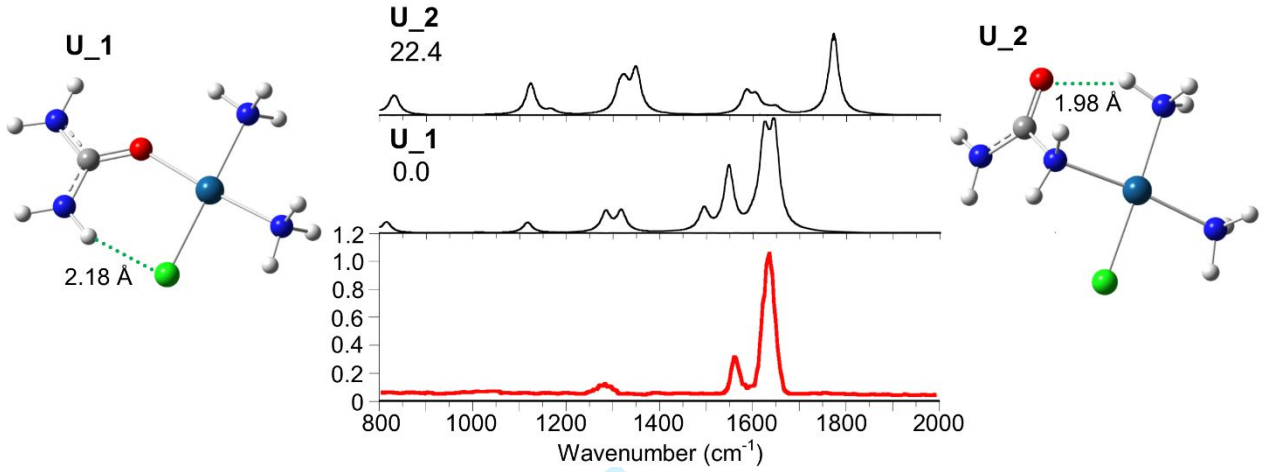

Fig. 3. IRMPD spectrum of *cis*-$[PtCl(NH_3)_2(Urea)]^+$ (red profile) compared with calculated harmonic IR spectra of **U_1** and **U_2** isomers optimized at the B3LYP/6-311+G(d,p) (Pt = LANL2TZ) level (black profiles). Relative free energy at 298 K, in kJ mol^{-1}, is given under each **U_1/2** label. Theoretical spectra are scaled by a 0.974 factor.

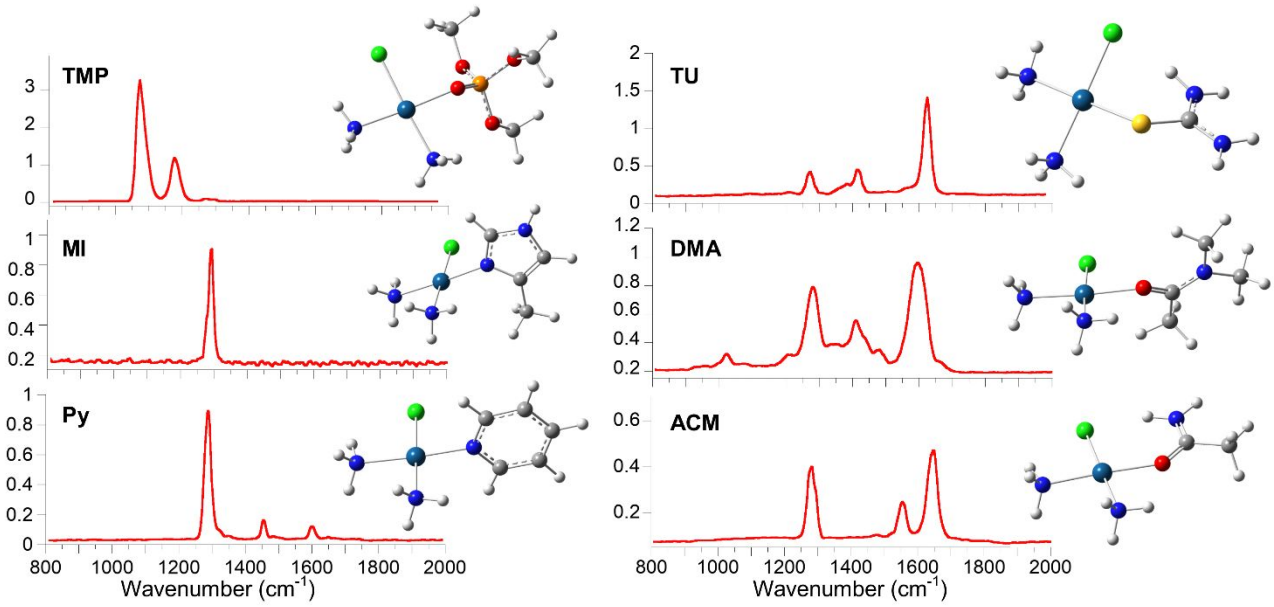

Fig. 4. IRMPD spectra of *cis*-$[PtCl(NH_3)_2(L)]^+$ complexes. Also shown are the structures assigned on the basis of the matching between IRMPD spectra and IR spectra of the optimized geometries at B3LYP/6-311+G(d,p) (Pt = Lanl2TZ) level of theory.

Cisplatin binding to an N-donor amino acid, histidine

The imidazole side group of histidine residues is a favored platination site as shown by several ESI MS and X-ray diffraction studies [8,46-48]. However, cisplating binding to a single L-histidine (His) molecule yields already a complex product pattern, depending on pH and evolving to multiply substituted and chelate complexes, so that the early primary complex deriving from reaction 1 (L = His) is not evidenced [49-50]. Favorably, the *cis*-$[PtCl(NH_3)_2(His)]^+$ complex is clearly identified in ESI MS, as shown in the spectrum reported in Fig. 5 [51]. The primary complex involving the cisplatin adduct where histidine has replaced a chlorido ligand corresponds to the isotopic cluster at *m/z* 418 (*m/z* of the first significant peak in the cluster is henceforth reported). The *cis*-$[PtCl(NH_3)_2(His)]^+$ species of interest may thus be examined for spectroscopic and reactivity properties to obtain structural information [51]. The ions at *m/z* 418 were sampled by collision induced dissociation (CID) at variable energy showing contrasting behavior. While at minimal collision energy already a considerable fraction of ions has undergone loss of NH_3, a sizeable portion is instead resistant to fragmentation even at high collision energy. This behavior suggests the presence of isomeric ions and in fact two families of isomers can be expected depending on the site of Pt binding. Fig. 6 displays the optimized structure of two regioisomers whereby platinum is ligated to an imidazole nitrogen being either N_π (pros, near) or N_τ (tele, far), in reference to their position relative to the side chain (**N_π_1**, **N_π_2**, **N_τ_1**, and **N_τ_2** are the most stable conformers).

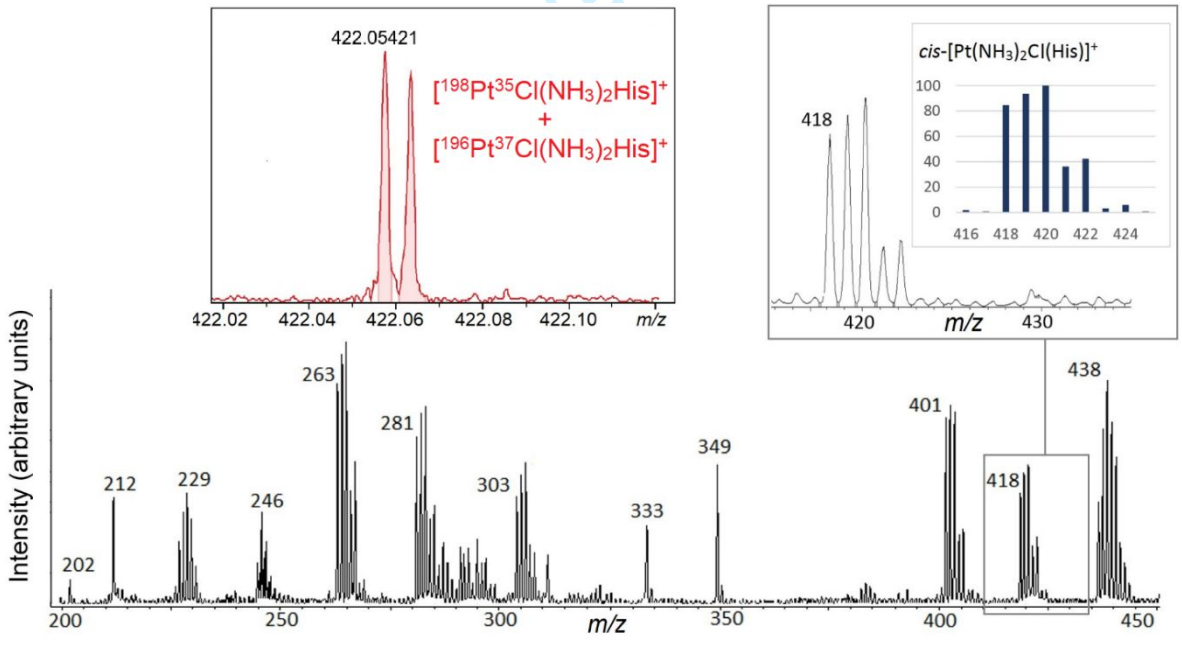

Fig. 5: Mass spectrum of a solution of cisplatin and His (1:1) 5×10^{-5} M in 50:50 methanol/water. The species of interest, the *cis*-$[PtCl(NH_3)_2His]^+$ complex, corresponds to the cluster at *m/z* 418. The assignment is consistent with the isotopic pattern enlarged in the inset, matching the calculated distribution (blue sticks) congruent with the presence of one platinum and one chlorine atom. High resolution FT-ICR mass spectra (an excerpt shown on the upper left panel) confirm the elemental composition.

The presence of both N_π and N_τ isomers explains the fragmentation behavior upon CID because only the N_π geometry may lead by NH_3 loss to a chelate complex where the metal is additionally bound to the amino N atom (N_a) ($[PtCl(NH_3)His(N_\pi,N_a)]^+$), the chelation motif also observed in aqueous solution [49]. Figure 6 displays also the computed IR spectra for **N_π_1**, **N_π_2**, **N_τ_1**, and **N_τ_2** which are compared with the experimental IRMPD spectrum to gain insight into the composition of the sampled ion population. The IRMPD spectrum shows that indeed an ion mixture is present, because none of the IR spectra matches alone the experimental features. The most informative part of the spectrum is the higher energy range where the prominent band at 3497 cm^{-1} is due to the NH stretching mode of the imidazole group which characterizes the IR spectra of **N_π** conformers. In the **N_τ** configuration the imidazole NH is engaged in hydrogen bonding, causing a red shift in the NH stretching frequency. The band at 3565 cm^{-1} arises from the OH stretching mode of a 'free' hydroxyl group, as verified in **N_π_2**, **N_τ_1** and **N_τ_2** isomers. These frequencies are isomer/conformer specific and thus lend themselves to be used for photofragmentation kinetics to probe the composition of the ion mixture [52].

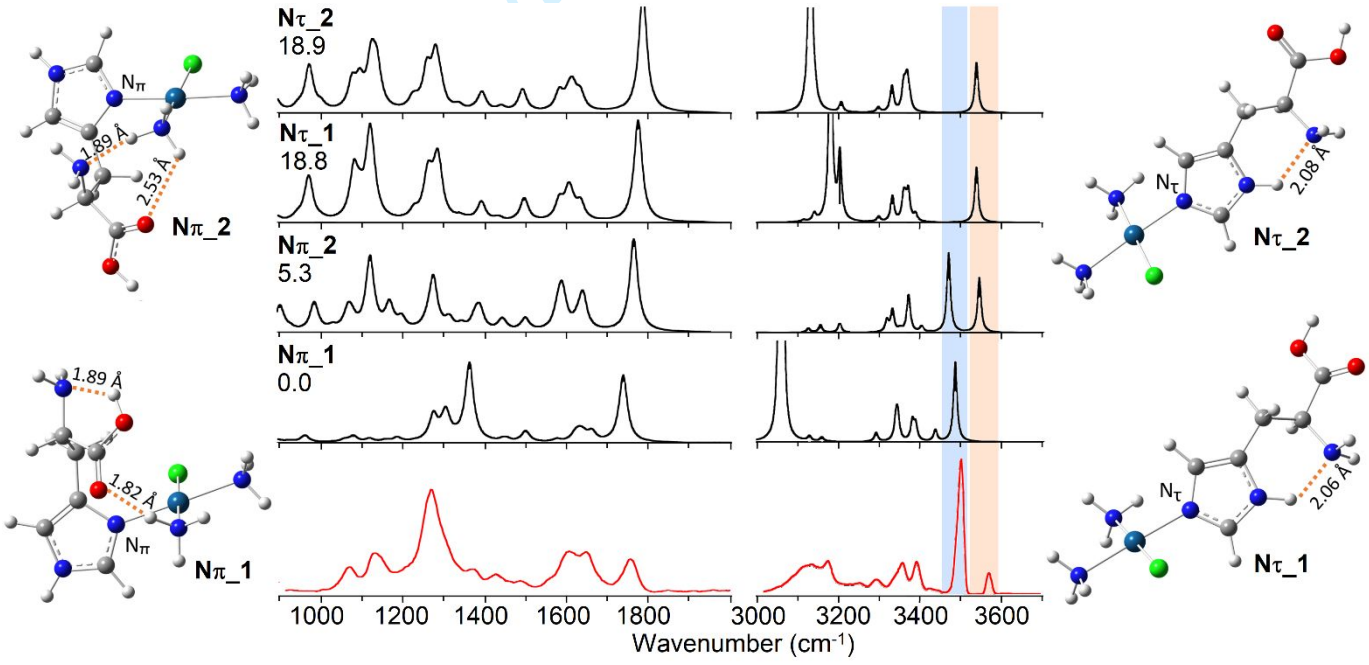

Fig. 6: IRMPD spectrum of *cis*-$[PtCl(NH_3)_2His]^+$ (red profile) compared to the unscaled linear anharmonic IR spectra calculated at B3LYP/6-311+G(d,p) (Pt = LANL2TZ) level for the most stable conformers of N_π and N_τ families of isomers (black profiles). Optimized geometries at the same level of theory are reported together with relative free energies at 298 K in kJ mol^{-1} calculated at the ωB97X-D/6-311+G(d,p) level.

IRMPD kinetics monitored at 3497 and 3565 cm^{-1} are shown in Fig. 7 reporting the decay of the parent ion *cis*-$[PtCl(NH_3)_2His]^+$ abundance as a function of irradiation time. For both kinetics a neat exponential decay is observed with rate constants differing by less than a factor of 2. This behavior is consistent with the presence of **N_π_1** and **N_π_2** conformers, endowed with comparable photofragmentation properties in the two resonances. The photofragmentation kinetics do not proceed to completion and an unreactive fraction is measured equal to 25% and 70% at 3497 and 3565 cm^{-1}, respectively. This finding is accounted for by

N_π_1 not being IR active at 3565 cm^{-1}, while the residual intact fraction at 3497 cm^{-1} is associated to **N_τ** conformers, displaying red-shifted imidazole NH stretch. However, the predicted red shift does not simply account by itself for the missing photofragmentation activity. In fact, this 25% residual intact fraction is also confirmed on other tested absorption frequencies that are commonly active for all **N_π/N_τ** isomers (for example at 3350 and 3392 cm^{-1}). This finding suggests that laser fluence in this frequency range is not adequate to activate **N_τ** species towards NH_3 cleavage, being the process relatively more unfavorable with respect to fragmentation from **N_π** complexes. NH_3 cleavage from **N_π** complexes may be assisted by the amino acid NH_2 group thus forming a chelate complex, a documented process in the platination of histidine in water solution [50]. This intramolecular ligand exchange process is prohibited by the geometry of **N_τ** complexes which yield an energetically high lying three coordinate complex upon release of NH_3. The inference is that the low fluence of the OPO/OPA laser used in this wavenumber range is inadequate to activate IRMPD of **N_τ** isomers. Thus, analysis of the collected data point out that **N_π_1**, **N_π_2**, and **N_τ_1 /N_τ_2** species are present in 45:30:25 ratio in the sampled mixture.

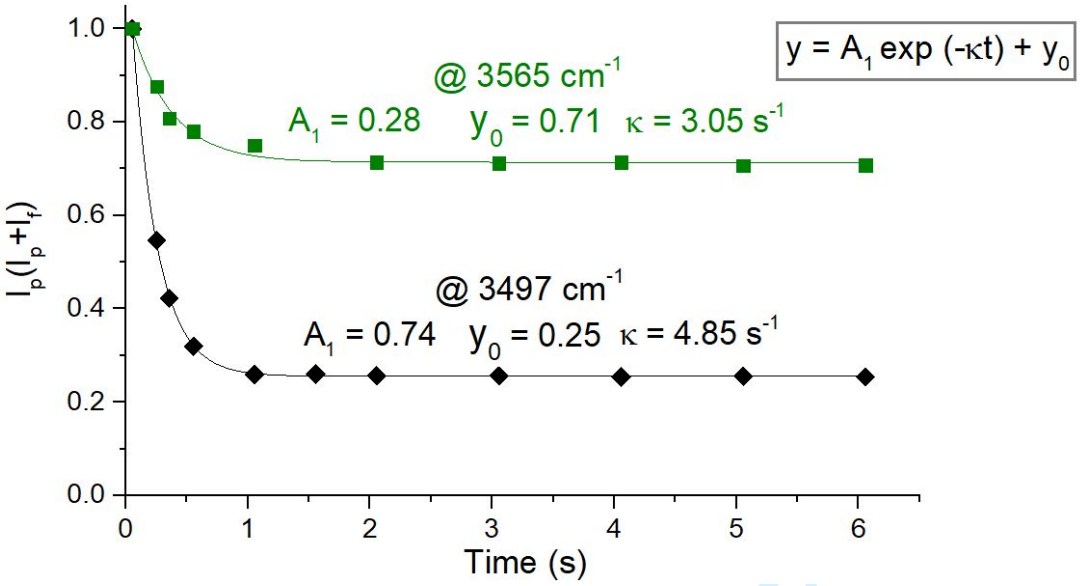

Fig. 7: Plot showing the decay of the parent ion *cis*-$[PtCl(NH_3)_2His]^+$ abundance as a function of irradiation time at two different wavenumbers. Fitting exponential functions are reported.

To summarize, in contrast with a previous report [53], ESI MS has successfully yielded *cis*-$[PtCl(NH_3)_2His]^+$ complexes, namely the primary species deriving from His binding to cisplatin or its monoaqua derivative. IRMPD spectroscopy has revealed a mixture of isomers formed by metal binding to either N_π or N_τ nitrogen of the imidazole side group. The relative fraction of N_π versus N_τ attack could be estimated by the amplitude of photofragmentation processes recorded on diagnostic resonances.

Cisplatin (and transplatin) binding to an S-donor amino acid, methionine

According to hard soft acid base (HSAB) theory, cisplatin, bearing a soft metal is predicted to have high affinity for sulfur containing ligands and in fact sulfur containing peptides and proteins are known to efficiently bind, performing also a transport role for the drug [9, 54-56]. When cisplatin is allowed to react

with methionine (Met), a complex product pattern is observed including both monofunctional and chelate species but, as in the case of His, the early complex displaying the first metal coordination event has not yet been characterized in solution. ESI has once again been used to deliver the ion of interest, $[PtCl(NH_3)_2Met]^+$ at *m/z* 412, formed by reaction of either cisplatin or transplatin, to be assayed for structural characterization [57]. However, typically informative tools in MS, such as CID mass spectra or methods based on ion mobility separation, discriminating ions according to different shape (collision cross section in a bath gas), do not make appreciable distinction between *cis*- and *trans*-$[PtCl(NH_3)_2Met]^+$. Vibrational ion spectroscopy provides the sought solution to the problem [57]. IRMPD spectra reported in Fig. 8 are clearly different for the two isomers, presenting several bands at closely similar frequency, though largely varying in intensity. One may notice, for example, a major band at 1130 cm^{-1} in the spectrum of the trans isomer which corresponds to an only weak one in the spectrum of the cis isomer, while an intense band for the cis complex at 1376 cm^{-1} has a weak counterpart for the trans at ca. 1367 cm^{-1}. However, in order to obtain thorough structural insight, as usual, one needs to explore potential geometries for the two isomers which best account for the recorded spectra.

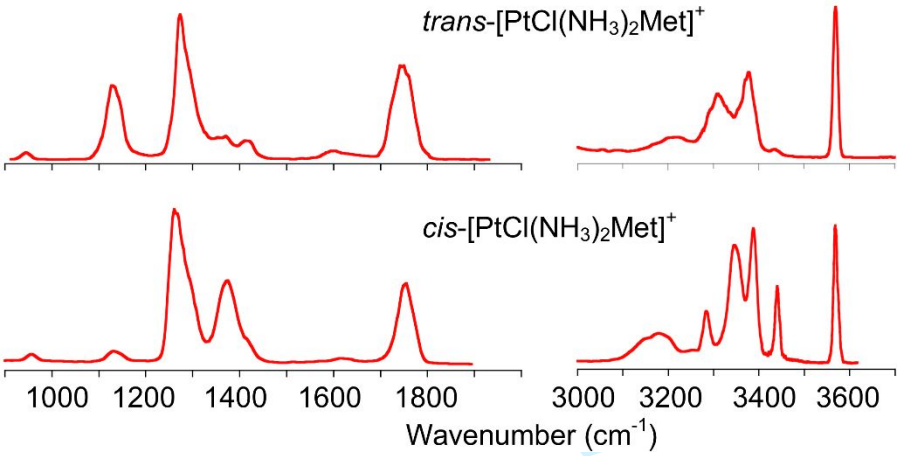

Fig. 8: IRMPD spectra of *cis*-$[PtCl(NH_3)_2Met]^+$ and *trans*-$[PtCl(NH_3)_2Met]^+$ complexes.

The most stable isomers for *cis*-$PtCl(NH_3)_2Met]^+$ complexes are presented in Fig. 9 together with the associated IR spectra. S-ligated complexes, **cS1** and **cS2** at 0 and 4 kJ/mol relative free energy, are more stable than N-ligated species, for example **cN1** at 18 kJ/mol.

Comparing the computed IR spectra with the experimental IRMPD spectrum suggests that the contribution of more than one geometry though a mixture of **cS1** and **cS2** may well explain the observed features. In particular, in the higher wavenumber range, **cS2** may be attributed the OH stretching band at 3564 cm^{-1}, due to the 'free' OH of the carboxylic group in syn configuration. The anti carboxylic group in **cS1** allows OH···NH_2 hydrogen bonding which causes the calculated O-H stretching to be shifted at 3083 cm^{-1}. However, a characteristic mode revealing the ligation motif is the asymmetric stretching of the α-amino group. This mode is responsible for the IRMPD band at 3443 cm^{-1}, corresponding to the calculated resonance appearing in the spectra of **cS** isomers. In contrast, IR activity is missing in the spectra of **cN** isomers at this frequency because platination at the NH_2 group as in **cN1** shifts the asymmetric NH_2 stretching to 3318 cm^{-1}. It may be noted that in both **cS1** and **cS2** isomers the NH_2 group is involved in

hydrogen bonding, the already cited OH···NH_2 interaction in **cS1** and HNH···O=C in **cS2** isomers, apparently affecting the asymmetric stretching wavenumber to a comparable extent.

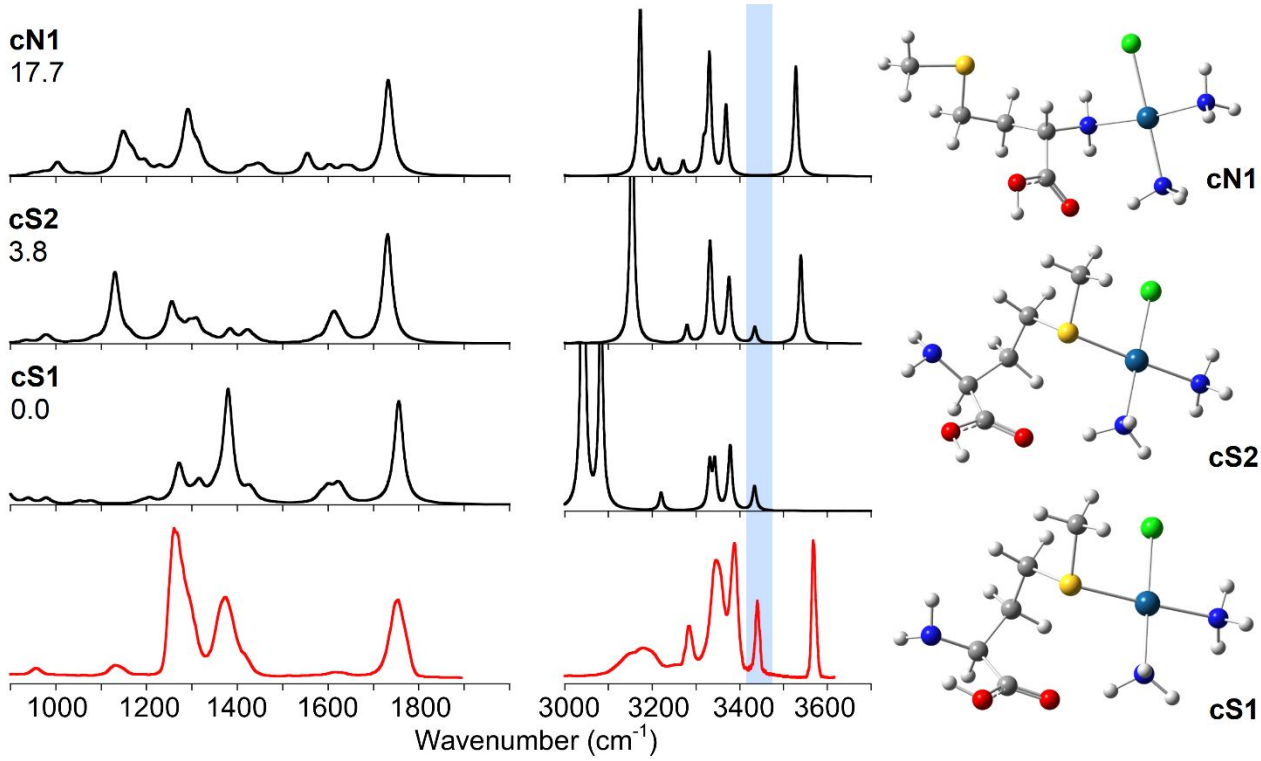

Fig. 9: IRMPD spectrum of *cis*-[PtCl(NH_3)$_2$Met]$^+$ (red profile), compared with calculated unscaled anharmonic spectra of selected isomers at the B3LYP/6-311++G(2df,pd) level using the 6-311++G(3df) basis set for S and the pseudopotential LANL2TZ-f for Pt. The corresponding optimized geometries are shown on the right. Relative free energies at 298 K in kJ mol^{-1} are reported.

trans-PtCl(NH_3)$_2$Met]$^+$ complexes present S- and N-ligated complexes that are more closely distributed in relative energy. Fig. 10 displays the lower lying conformers **tN1**, **tS1** and **tS2**, collectively contributing to the recorded IRMPD spectrum. In this spectrum the band at 3434 cm^{-1}, recognized to pertain to the asymmetric stretching of the α-amino group and as such appearing as a major feature in the IR spectra of **tS1** and **tS2**, is noticeably weaker when compared with the corresponding one in the spectrum of the cis isomer. This evidence and the similar energy of **tS** and **tN** isomers support a comparable contribution of the two families of complexes in the sampled ions. However, a semiquantitative evaluation is afforded by photofragmentation kinetics at the diagnostic NH_2 asymmetric stretching at 3443/3434 cm^{-1} in the IRMPD spectra of *cis*- and *trans*-[PtCl(NH_3)$_2$Met]$^+$ complexes, respectively.

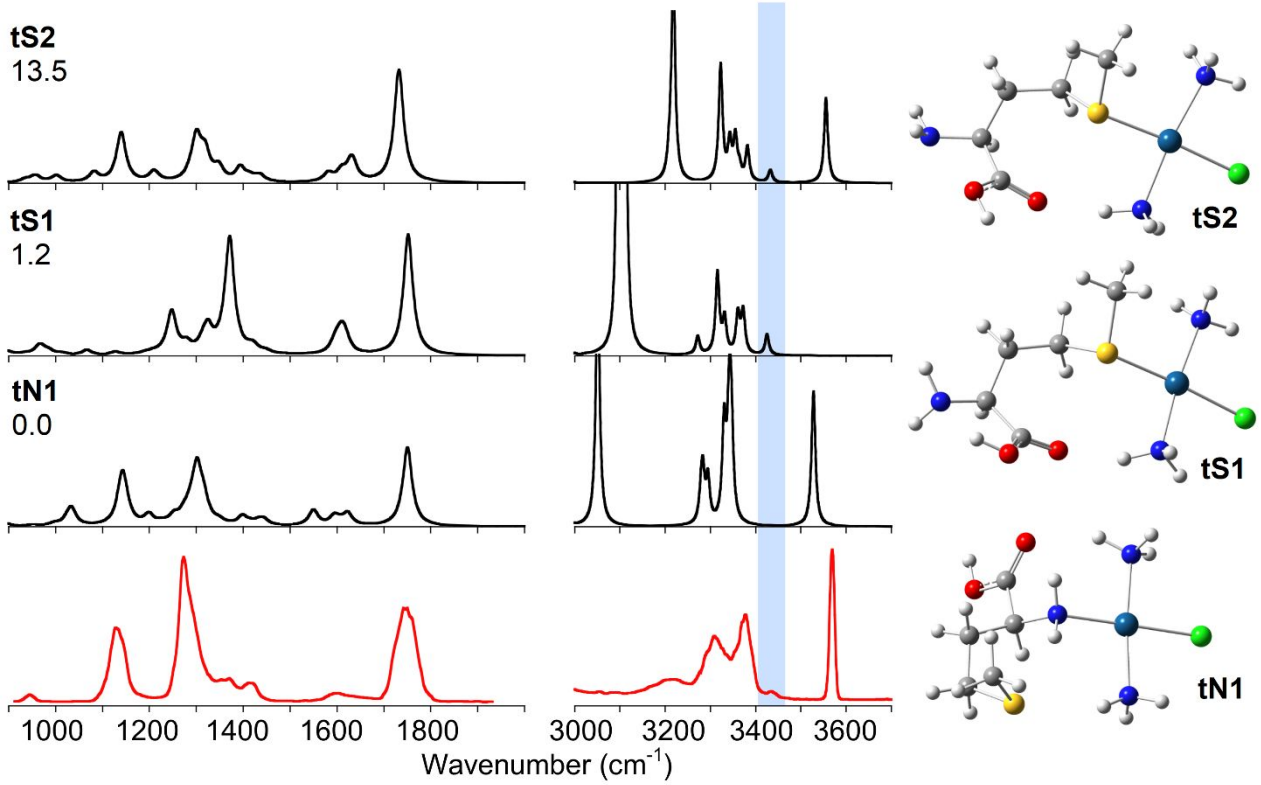

Fig. 10: IRMPD spectrum of *trans*-[PtCl(NH_3)$_2$Met]$^+$ (red profile), compared with calculated unscaled anharmonic spectra of selected isomers at the B3LYP/6-311++G(2df,pd) level using the 6-311++G(3df) basis set for S and the pseudopotential LANL2TZ-f for Pt. The corresponding optimized geometries are shown on the right. Relative free energies at 298 K in kJ mol^{-1} are reported.

The exponential plots reported in Fig. 11 do not differ significantly in terms of time constant but considerably more in the amplitude of the process. In fact, the photofragmentation leaves an unreactive fraction of *trans*-isomer of ca. 64% while the process goes almost to completion for *cis*-[PtCl(NH_3)$_2$Met]$^+$. It may be thus inferred that cisplatin preferentially reacts at the thiomethyl group whereas transplatin is less selective yielding also N-coordination. A rationale for the different behavior may be ascribed to the trans influence in square planar platinum(II) complexes. In fact, in the case of transplatin, S-platination leads to a complex whereby two donating groups with rather high trans influence (thiomethyl and chloride) are placed in trans relationship to each other, competing for donation and destabilizing the complex [12,39,58]. Under these circumstances, the typically favored S-attack becomes relatively disfavored.

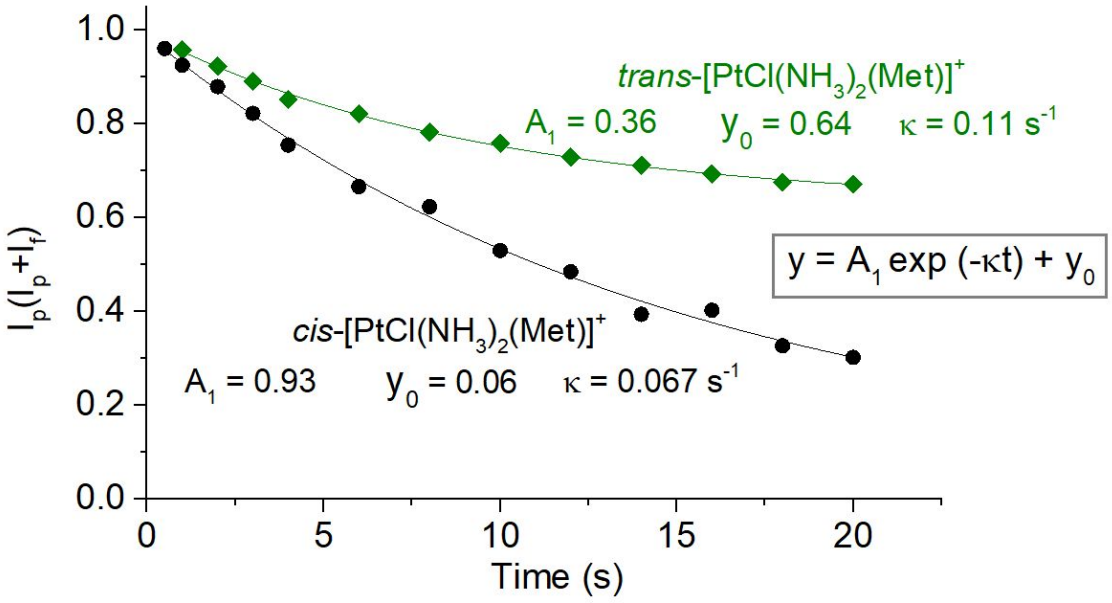

Fig. 11: Plots showing the decay of the relative abundancies of the sampled ions, *cis*- and *trans*-$[PtCl(NH_3)_2Met]^+$, as a function of the irradiation time. Fitting exponential functions are reported.

Conclusions

Electrospray ionization coupled to mass spectrometry and IR laser spectroscopy combined with quantum chemical calculations have released structural insight on the early complexes involved in the biological fate of cisplatin or on simple models thereof. The initial active species are obtained by an aquation process replacing the chlorido ligand(s) and IRMPD spectroscopy has revealed the vibrational features of *cis*- and *trans*-$[PtX(NH_3)_2(H_2O)]^+$ (X = Cl, OH) complexes. Cisplatin undergoes ligand substitution with simple molecules mimicking biological targets in aqueous solution yielding, *cis*-$[PtCl(NH_3)_2L]^+$ (X = Py, MeIm, TA, TMP, ACM, DMA, U, and SU) complexes. These complexes, assayed by IRMPD spectroscopy, have shown regioselective platination in the presence of potentially competing sites (for example the carbonyl oxygen of U or the phosphoryl oxygen of TMP). Histidine and methionine (together with cysteine) residues are the main Pt anchoring sites within peptides and proteins. IRMPD spectroscopy and photofragmentation kinetics have allowed us to obtain a detailed cisplatin coordination pattern yielding information on both binding regioselectivity and also on the most favored conformers in each family of isomers (for example within N_π and N_τ isomers in His complexes). It may be underlined that the observed binding motifs of cisplatin with the sampled bioligands concern substitution products formed in aqueous solution and sampled in the gas phase. Indeed, any isomerization involving breaking and rearrangement of coordination bonds to the metal is inhibited by high activation energies in the gaseous isolated species [51,57]. However, the reaction with the free sampled amino acids may bear consequence on the platination of proteins in biological media. In fact, according to reported X-ray diffraction studies and MS investigations, Pt binding involves mainly solvent exposed protein side chains [7,55]. The present contribution may thus provide a useful reference for the plain early platination event occurring in the aqueous medium from where the sampled ionic complexes are extracted and isolated.

Acknowledgments: This research was supported by the Università degli Studi di Roma La Sapienza and by the European Commission (CLIO project IC14-011).
The authors are grateful to Philippe Maitre, Jean-Michel Ortega, Debora Scuderi, Vincent Steinmetz and the CLIO team and to Annito Di Marzio for experiments at the OPO/OPA laser.

REFERENCES

[1] B. Rosenberg, L. V. Camp, J. E. Trosko, V. H. Mansour. *Nature* **222**,385 (1969).
[2] R. A. Alderden, M. D. Hall, T. W. Hambley. *J. Chem. Ed.* **83**, 728 (2006).
[3] D. Wang, S. J.Lippard. *Nat. Rev. Drug Discov.* **4**, 307 (2005).
[4] J. Kozelka, F. Legendre, F. Reeder, J.-C. Chottard. *Coord. Chem. Rev.* **190-192**, 61 (1999).
[5] A. V. Klein, T. W. Hambley. *Chem. Rev.* **109**, 4911 (2009).
[6] B. Lippert. *Cisplatin: Chemistry and Biochemistry of a Leading Anticancer Drug*, Wiley-VCH, Zurich, Switzerland (1999).
[7] A. Merlino, T. Marzo, L. Messori. *Chem. Eur. J.* **23**, 6942 (2017).
[8] A. Casini, J. Reedijk. *Chem. Sci.* **3**, 3135 (2012).
[9] H. Li, Huilin,Y. Zhao, H. I. A. Phillips, Y. Qi, T.-Y Lin, P. J. Sadler, P. B. O'Connor. *Anal. Chem.* **83**, 5369 (2011).
[10] Z. D. Bugarcic, J. Bogojeski, B. Petrovic, S. Hochreuther, R. van Eldik. *Dalton Trans.* **41**, 12329 (2012).
[11] D. V. Deubel. *J. Am. Chem. Soc.* **126**, 5999 (2004).
[12] D. T. Richens. *Chem. Rev.* **105**, 1961 (2005).
[13] S. J. Berners-Price, T. G. Appleton. *The chemistry of cisplatin in aqueous solution.* In *Platinum-based drugs in cancer therapy. Cancer drug discovery and development* (L. R. Kelland, N. P. Farrell eds.), pp. 3-35. Humana Press, Totowa, NJ (2000).
[14] J. Vinje, E. Sletten, J. Kozelka. *Chem. Eur. J.* **11**, 3863 (2005).
[15] S. J. Lippard. *Science* **218**, 1075 (1982).
[16] S. Hochreuther, R. Puchta, R. van Eldik. *Inorg. Chem*. **50**, 12747 (2011).
[17] Z. Xu, J. S. Brodbelt. *J. Am. Soc. Mass Spectrom.* **25**, 71 (2014).
[18] L. A. Hammad, G. Gerdes, P. Chen. *Organometallics* **24**, 1907 (2005).
[19]M. Cui, L. Ding, Z. Mester. *Anal. Chem*. **75**, 5847 (2003).
[20] M. L. Styles, R. A. J. O'Hair, W. D. McFadyen, L. Tannous, R. J. Holmes, R. W. Gable. *J. Chem. Soc., Dalton Trans.* **0**, 93 (2000).
[21] J. Oomens, B. G. Sartakov, G. Meijer, G. von Helden. *Int. J. Mass Spectrom.* **254**, 1 (2006).
[22] L. MacAleese, P. Maitre. *Mass Spectrom. Rev.* **26**, 583 (2007).
[23] L. Jašíková, J. Roithová. *Chem. Eur. J.* **24**, 3374 (2018).
[24] T. D. Fridgen. *Mass Spectrom. Rev.* **28**, 586 (2009).
[25] J. R. Eyler. *Mass Spectrom. Rev.* **28**, 448 (2009).
[26] N. C. Polfer, J. Oomens. *Mass Spectrom. Rev.* **28**, 468 (2009).
[27] N. C. Polfer. *Chem. Soc. Rev.* **40**, 2211 (2011).
[28] M. Katari, E. Payen de la Garanderie, E. Nicol, V. Steinmetz, G. van der Rest, D. Carmichael, G. Frison. *Phys. Chem. Chem. Phys.* **17**, 25689 (2015).
[29] B. Chiavarino, M. E. Crestoni, S. Fornarini, S. Taioli, I. Mancini, P. Tosi. *J. Chem. Phys.* **137**, 024307 (2012).
[30] A. Ciavardini, A. Dalla Cort, S. Fornarini, D. Scuderi, A. Giardini, G. Forte, E. Bodo, S. Piccirillo. *J. Mol. Spectrosc.* **335**, 108 (2017).
[31] R. C. Dunbar, J. Martens, G. Berden, J. Oomens. *Int. J. Mass Spectrom.* **429**, 198 (2018).
[32] A. M. Chalifoux, G. C. Boles, G. Berden, J. Oomens, P. B. Armentrout. *Phys. Chem. Chem. Phys.* **20**, 20712 (2018).
[33] K. Peckelsen, J. Martens, G. Berden, J. Oomens, R. C.Dunbar, A. J.H.M.Meijer, M.Schäfer. *J. Mol. Spectrosc.* **332**, 38 (2017).
[34] B. E. Ziegler, R. A. Marta, M. B. Burt, T. B. McMahon. *Inorg. Chem.* **53**, 2349 (2014).

[35] T. E. Hofstetter, C. Howder, G. Berden, J. Oomens, P. B. Armentrout. *J. Phys. Chem. B* **115**, 12648 (2011).
[36] A. De Petris, A. Ciavardini, C. Coletti, N. Re, B. Chiavarino, M. E. Crestoni, S. Fornarini. *J. Phys. Chem. Lett.* **4**, 3631 (2013).
[37] D. Corinti, C. Coletti, N. Re, S. Piccirillo, M. Giampà, M. E. Crestoni, S. Fornarini. *RSC Adv.* **7**, 15877 (2017).
[38] C. C. He, B. Kimutai, X. Bao, L. Hamlow, Y. Zhu, S. F. Strobehn, J. Gao, G. Berden, J. Oomens, C. S. Chow, M. T. Rodgers. *J. Phys. Chem. A* **119**, 10980 (2015).
[39] Z.Chval, M. Sip, J. V. Burda. *J. Comput. Chem.* **29**, 2370 (2008).
[40] B. Chiavarino, M. E. Crestoni, S. Fornarini, D. Scuderi, J.-Y. Salpin. *Inorg. Chem.* **56**, 8793 (2017).
[41] B. Chiavarino, M. E. Crestoni, S. Fornarini, D. Scuderi, J.-Y. Salpin. *Inorg. Chem.* **54**, 3513 (2015).
[42] B. Chiavarino, M. E. Crestoni, S. Fornarini, D. Scuderi, J.-Y. Salpin. *J. Am. Chem. Soc.* **135**, 1445 (2013).
[43] D. Corinti, C. Coletti, N. Re, B. Chiavarino, M. E. Crestoni, S. Fornarini. *Chem. Eur. J.* **22**, 3794 (2016).
[44] D. Corinti, C. Coletti, N. Re, R. Paciotti, P. Maitre, B. Chiavarino, M. E. Crestoni, S. Fornarini. *Int. J.Mass Spectrom.* **435**, 7 (2019).
[45] M. S. Davies, S. J. Berners-Price, T. W. Hambley. *Inorg. Chem.* **39**, 5603 (2000).
[46] V. Calderone, A. Casini, S. Mangani, L. Messori, P. L. Orioli. *Angew. Chem.* **45**, 1267 (2006).
[47] H. Li, Y. Zhao, H. I. A. Phillips, Y. Qi, T.-Y. Lin, P. J. Sadler, P. B. O'Connor. *Anal. Chem.* **83**, 5369 (2011).
[48] A. Casini, A. Guerri, C. Gabbiani, L. Messori. *J. Inorg. Biochem.* **102**, 995 (2008).
[49] V. Saudek, H. Pivcova, D. Noskova, J. Drobnik. *J. Inorg. Biochem.* **23**, 55 (1985).
[50] T. G. Appleton. *Coord. Chem. Rev.* **166**, 313 (1997).
[51] D. Corinti, A. De Petris, C. Coletti, N. Re, B. Chiavarino, M. E. Crestoni, S. Fornarini. *ChemPhysChem* **18**, 318 (2017).
[52] J. S. Prell, T. M. Chang, J. A. Biles, G. Berden, J. Oomens, E. R. Williams. *J. Phys. Chem. A* **115**, 2745 (2011).
[53] H. Liu, N. Zhang, M. Cui, Z. Liu, S. Liu. *Int. J. Mass Spectrom.* **409**, 59 (2016).
[54] J. Reedijk. *Chem. Rev.* **99**, 2499 (1999).
[55] L. Messori, A. Merlino. *Coord. Chem. Rev.* **315**, 67 (2016).
[56] C. M. Sze, G. N. Khairallah, Z. Xiao, P. S. Donnelly, R. A. J. O'Hair and A. G. J. Wedd, *J. Biol. Inorg. Chem.*, **14**, 163 (2009).
[57] R. Paciotti, D. Corinti, A. De Petris, A. Ciavardini, S. Piccirillo, C. Coletti, N. Re, P. Maitre, B. Bellina, P. Barran, B. Chiavarino, M. E. Crestoni, S. Fornarini. *Phys.Chem. Chem. Phys.* **19**, 26697 (2017).
[58] B. Pinter, V. Van Speybroeck, M. Waroquier, P. Geerlings, F. De Proft. *Phys. Chem. Chem. Phys.* **15**, 17354 (2013).